EFFECT OF STRETCHING STIMULATION DURING CULTURE ON MENISCAL ENTHESIS CONSTRUCTS

A Thesis

Presented to the Faculty of the Graduate School

of Cornell University

In Partial Fulfillment of the Requirements for the Degree of

Master of Science in Material Science and Engineering

by

Xun Wang

December 2021

ABSTRACT

Tissue engineered (TE) menisci have been seen as a very promising treatment for meniscus injury repair in human knee joints. Although much effort has been focused on the TE meniscus body, less attention has been paid to the connective integration between the meniscus and the underlying bone, which plays a significant role in the mechanical stability and the success rate of meniscal repair. This specific connective tissue in the knee joint is called the meniscal enthesis. In this research, a simplified meniscal enthesis construct model is used as a platform for experiments and testing to mimic the complex native enthesis structure. The model is composed of a collagen gel with fibrochondrocytes (meniscus region), decellularized bone plugs (bone region), and an interface region. Stretching stimulation along the axial direction has been applied onto clamped meniscal enthesis constructs during culture as an attempt to improve the mechanical performance and collagen fiber organization. For the realization of the stretching function, a bioreactor was designed and produced using 3D printing technique with polylactic acid (PLA) material. After 4 weeks of culture on the bioreactors, tensile testing and histology analysis were applied onto the constructs for exploration of potential effect of stretching during culture. As a result, the 3D printed bioreactor successfully realized the stretching function on meniscal enthesis constructs. Stretched constructs showed more longitudinal fiber bundles while less radial ones. Stretching stimulation also increased the strain of failure while decreased the tensile modulus and ultimate tensile stress of the constructs. For further research,

parameters like stretching rate, culture time before stretching and directions of loading should be considered for improvement of fiber organization and mechanical properties of meniscal enthesis constructs.

BIOGRAPHICAL SKETCH

Xun Wang was born in 1995 in Zhenjiang, a city in Jiangsu Province, China. Influenced by his father who had been an engineer, Xun showed an interest in nature science and engineering from a young age. This led to his academic career in engineering and science research. He achieved his Bachelor's degree of Science in Engineering in the school of Material Science & Engineering from Shanghai Jiao Tong University in 2018. During his undergraduate studies he joined Professor Li, Wanwan's group, and participated in the research of AIE fluorescent encoded nanospheres. He systematically started his career as a researcher and learned how to find, analyze, finally, dissolve a problem as a material scientist and engineer. After graduation, he worked as a research assistant in the same lab for half a year and expanded his researching to quantum dots. The charm of scientific research fascinated him and made him decide to apply for MS degree for further learning.

Xun started his Master program in Material Science and Engineering in Cornell University in 2019. There, he joined the meniscus group, co-advised by Dr. Lara Estroff and Dr. Lawrence Bonassar and began his touch with tissue engineering. Detailed guidance from advisors and group members have helped him step into this brand new field successfully. He designed and printed out the bioreactor for stretching with Sean and Jared's help, based on the linear meniscal enthesis constructs. He also explored the effect of mechanical stimulation during culture towards the connecting integrity and fiber organization of the constructs.

ACKNOWLEDGMENTS

I want to express my sincere thanks and gratefulness to everyone who has helped me during my 2-year study and research in Cornell University, especially my advisors, Professor Lara Estroff and Professor Lawrence Bonassar. It is not only their professional guidance that helps me successfully realize my scientific research idea, but also their rigorous and serious scientific attitudes and excellent personal characters that let me see what a qualified scientist and engineer should be like.

I also want to thank Jongkil Kim, Marianne Lintz, Leigh Slyker, Serafina Lopez, and Tianyu Gao for training me through all the techniques and steps during my research. Especially JK, thank you for your careful guidance and encouragement that helps me go through my toughest period. Sera, thank you for your help with four control sample data. For Sean Kim and Jared Matthews, thank you so much for helping me with the bioreactors design. And I want to thank all members in Bonassar's group and Estroff's group for your suggestions and support.

Finally, I want to thank my parents for respecting my decision to study abroad and funding me throughout my program. It is you that are always my strongest supporting behind me and making me get this far.

TABLE OF CONTENTS

LIST OF TABLES

LIST OF FIGURES

CHAPTER 1. INTRODUCTION AND BACKGROUND

1.1 Meniscus and Enthesis

The human meniscus is a cartilage structure that is located between the femur (thighbone) and tibia (shinbone) in the knee joint. The term ‘meniscus’ originates from the Ancient Greek word μηνίσκος (meniskos), which means "crescent"[1]. It describes the crescent shape of meniscus’ unique anatomical structure. The structure of meniscus is also described as semi-annular or half-moon with a thick periphery and a thin inner margin. The superior surface is concave, adapting to the femoral condyle, and the interior surface is flat, which fits the tibial plateau. There are two menisci in each human knee, which are the lateral meniscus and the medial meniscus (Figure 1.1.1). The function of the meniscus can be described as a stabilizer, lubricator and load distributor in the knee joint[2]. A normal meniscus can pad the internal and external condyles of the femur to increase joint stability. It also avoids the direct contact between femur and tibia and reduces the friction during movement. Owning to its particular biochemical composition and structure, the meniscus plays a significant role in improving joint congruity, handling load transmission, and absorbing shocks[3]. Because of these specific functions, meniscus health is important in our daily exercise and life.

Figure 1.1.1. Lateral(left) and medial(right) menisci, harvested from 1-3 day old bovids.

The enthesis structure generally refers to the connective tissue between soft tissue like ligament or tendon, and bone[4]. There are mainly two types of entheses which are the fibrous and the fibrocartilaginous entheses[5,6]. Fibrous entheses are composed of dense fibrous tissue and the soft tissue directly attaches to the bone.

1.2 Meniscus Injury and Treatment

As one of the key mechanical tissues in human knee joints, meniscus plays an important role in our daily life. At the same time, however, the meniscus is a very fragile structure, and meniscus injuries are also very common in knee joint injuries. Basically, any activities that involve overstretching, twisting, rotation or sudden pressure in the knee joint during our normal exercises can result in

meniscus injury. Swelling and stiffness are common symptoms of meniscus injuries. Patients may also experience pain in the knee joints especially when twisting and rotating, and difficulty in fully straightening their knees. It is reported that injuries or loss of meniscus will increase the contact pressure in the knee joints and result in osteoarthritis (OA)[7,8]. OA is one of the diseases in adults and about 237 million people all over the globe suffer from it[9,10].

At present, the treatments towards meniscus injury are partial meniscectomy, surgery repair and meniscal allograft[11]. Although partial removal of the injured meniscus can generally relieve symptoms, the amount of removed tissue is highly related to the degree of recovery of meniscus function and mechanical stability after the meniscectomy. It can also result in uneven load distribution and loss of normal meniscus function in knee joints. Surgery repairing can reduce pain and help recover meniscus function. It is reported that the successful rate of surgery repairing at the outer edge of meniscus, which is called the red zone, is 85%[12]. However, this method is limited by the location of injury. The repairing effect could be poor if the injury takes place at the center part of meniscus, which is called the white zone of meniscus. For meniscal allograft, patients are still suffering from lack of donor tissue and mismatched geometry between donors and patient. Therefore, the tissue engineered (TE) meniscus has been seen and spurred as a promising treatment towards meniscus injury in the near future.

1.3 Tissue Engineered Meniscal Enthesis Model

As a new promising technique for meniscus injury repairing, TE meniscus has lots of advantages compared with current options. This technique involves the use of differentiated or stem cells and different materials for scaffold[13,14]. Additionally, this technique will no be longer limited by the number of donors in allograft. The geometry shape and size of a TE meniscus can also be created according to the patient's knee joint. At present, many methods have been used for TE meniscus, which provides a new idea for repairing meniscus injury[15].

Previously, study and research are mainly focused on the creation of TE meniscus body[16]. For example, Alexander et al.[17] designed and 3D printed polycaprolactone (PCL) scaffolds that recapitulate the structural features of native meniscus extracellular matrix. The PCL scaffolds are used as a template and structural support for meniscus regeneration. This biomimetic scaffold provides a promising model for tissue engineered meniscus. However, not much effort and attention was concentrated onto the connective tissue between the meniscus body and underlying bone, which is the meniscal enthesis structure. In fact, the meniscus' function of relieving pressure on the tibia is closely related to the attachment to the bone part[18]. And the fixation of meniscus into the bone is of great significance for the success of meniscus repairing in the long term. In meniscus allograft, bone plugs or bone bridges are usually attached with the meniscus graft to maintain the firm connection between meniscus and underlying bone and to ensure the success of transplanting. While for TE meniscus, little efforts are paid onto this structure.

In this research, a simplified tissue engineered meniscal enthesis model is used to mimic the structure of native meniscal enthesis as a researching tool and testing platform. It has been verified as effective to mimic the native meniscal enthesis structure in former research and used for further understanding the connective integration between the soft tissue and bone tissue.

Anatomically, the meniscal enthesis structure has a gradient transition from fibrocartilage tissue to bone tissue. This transition structure can be divided into 4 different areas, which are the ligamentous zone, uncalcified fibrocartilage zone, calcified fibrocartilage zone and bone, from meniscus to bone in order[19-21] (Figure 1.3.1). Cell phenotype and collagen type vary within these 4 zones: For the ligamentous zone, it mainly contains fibroblasts and collagen type I, which is presented as highly aligned fiber bundles. While in the uncalcified fibrocartilage zone, we can find fibrochondrocytes, chondrocytes, proteoglycans and collagen type II, which is not aligned. Hypertrophic condrocytes and collagen II and X can be found in the calcified fibrocartilage zone. The bone region is composed of osteoblasts, osteoclasts, and osteocytes. The collagen within is mainly type I. In addition, the mechanical environment of this structure in human knee joint is also very complex. Not only does it absorb and distribute the compressive stress that comes from our daily life exercise, but it is also subjected to the tensile forces which hold it firmly into the underlying bone. All of these factors have greatly increased the difficulty of researching the meniscal enthesis constructs.

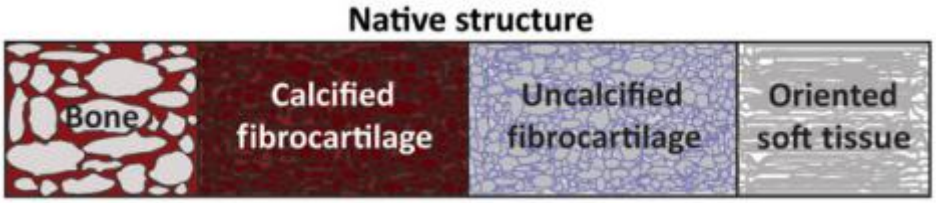

Figure 1.3.1. Schematic representation of the four different regions of the native meniscal enthesis structure. From reference 21.

Accordingly, the TE meniscal enthesis model we use in this research has simplified the complex meniscal enthesis structure into a linear model with three main zones: the collagen part (soft tissue zone), the bone part (hard tissue zone) and the interface between them. These zones are respectively used to mimic the meniscus, the underlying bone and the meniscal enthesis structure. It is generated through injecting collagen containing fibrochondrocytes into Tygon® tube with an inner diameter of 6 mm. And there are decellularized bone plugs set at both ends of the tube. After gelation, the bone-interface-collagen structure will be produced (Figure 1.3.2). This design of model has largely avoided the complex gradients of native meniscus structure and allows us to focus on the integration between the meniscus and underlying bone.

Figure 1.3.2. Three zones (bone zone, interface zone and collagen zone) of tissue engineered meniscal enthesis mold. Figure from reference 2.

1.4 Effects of Mechanical Stimulation to Tissue Culture

Mechanical loading environment is a critical component of any biological models during the process of scaffold culture. It is of great significance in functions like stimulating biosynthesis by cells and promoting molecular transport[22]. Cells under specific loading environment in tissue engineered scaffolds during culture can sense the environmental stimulation and transfer the mechanical stimulation into intracellular signaling. According to different loading stimuli, cells will make different responses and behaviors. These responses depend on different factors of mechanical stimuli like loading type, rate, magnitude and duration[22].

Based on this theory, many studies have introduced mechanical stimuli in an attempt to induce cellular behavior and improve the performance of TE scaffold. For example, an organ culture loading system is designed and applied for human or bovine intervertebral disc (IVD)[22] (Figure 1.4.1). This system provides a periodic dynamic mechanical stimulation environment for *in vitro* IVD culture to mimic the mechanical loading environment *in vivo*. The cells in the IVDs remained viable in

this system for culture up to 21 days. Also, this loading system provides a potential method and platform for further understanding and research of IVD.

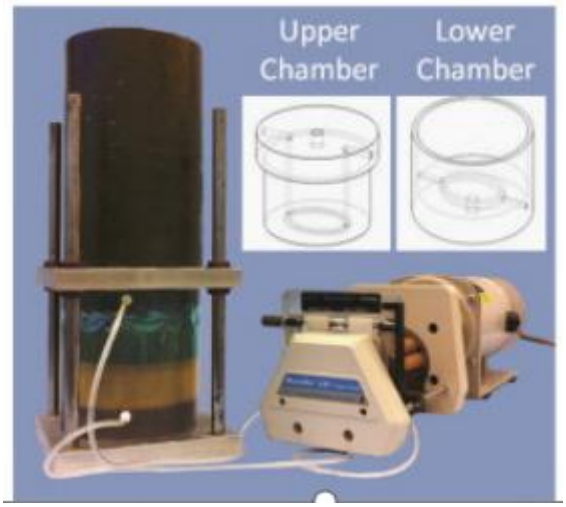

Figure 1.4.1. The culture system and culture chamber used for human IVD culture. From reference 22.

Mechanical stimulation has also been applied on the meniscal enthesis model (Figure1.3.2). One example is the research of effect on mechanical stimulation of clamping at bone plug ends onto bioreactors during culture[2]. In this research, meniscal enthesis constructs are clamped onto polysulfone molds for fixation during culture as experimental groups, unclamped enthesis constructs as control (Figure 1.4.2 A). After 28 days (4 weeks) of culture, it turns out that the collagen alignment and organization can be directed by using the method of clamping (Figure 1.4.3). Clamped meniscal enthesis constructs show improved mechanical properties compared with unclamped constructs (Figure 1.4.2 B). The elastic modulus has been significantly increased by 500% and UTS by 400% in clamped samples while it only increased by 150% in elastic modulus and 250% in UTS in unclamped constructs after 4 weeks. In summary, it proves that static

mechanical clamping during culture of the TE meniscal enthesis constructs successfully improves the structuring of the collagen fiber networks, especially close to the interface with the bony region. It also shows that this experimental model successfully provides a researching tool and platform for TE meniscal enthesis.

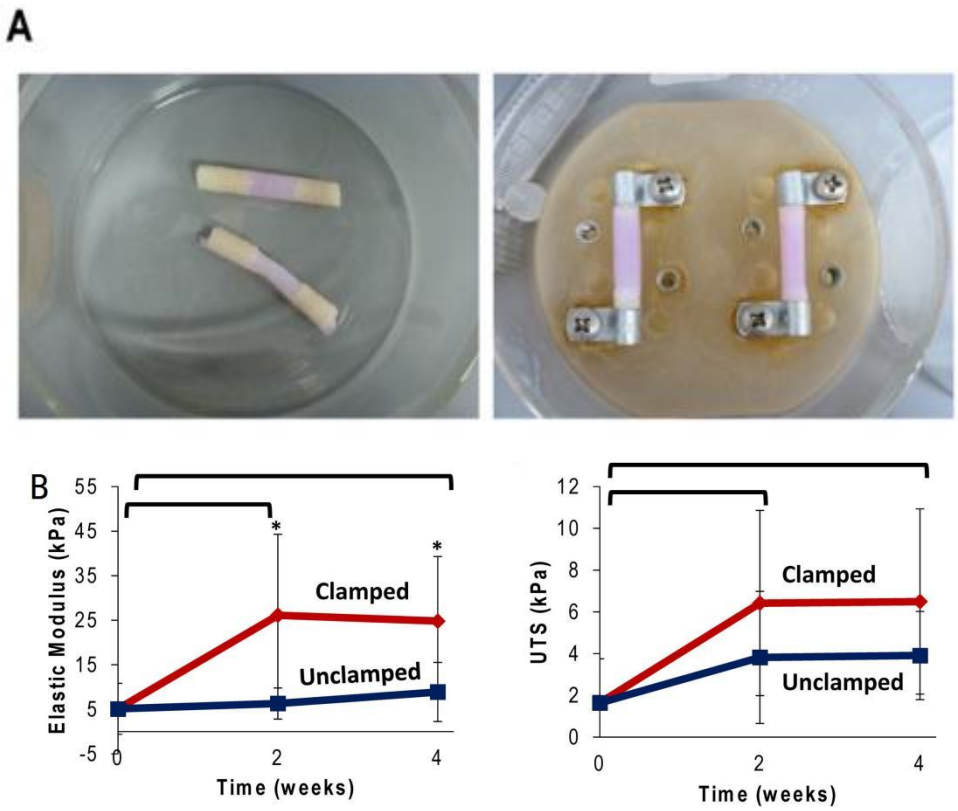

Figure 1.4.2 A. Unclamped meniscal enthesis constructs as control group (left) and clamped constructs as experimental group (right). B. Elastic Modulus and UTS of clamped and unclamped meniscal enthesis constructs after 28 days of culture. From reference 2.

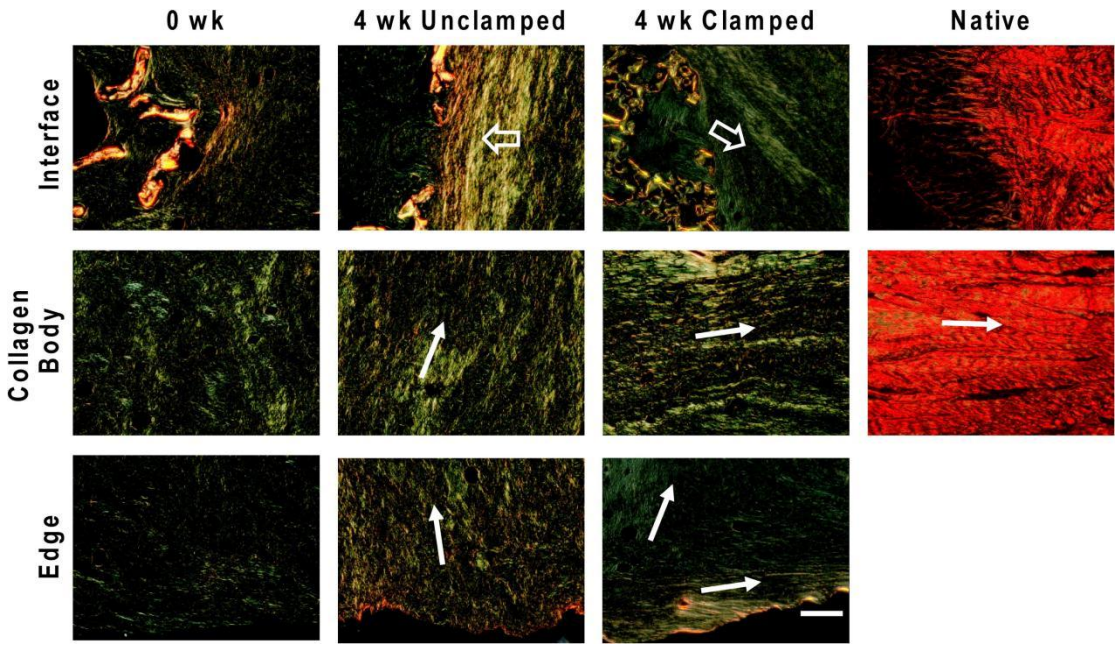

Figure 1.4.3. Picrosirius red staining images with polarized light of meniscal enthesis constructs from unclamped and clamped groups. The far right column shows images of native meniscal enthesis. Interfaces are pointed out by (=>). Fiber directions are indicated by (→). From reference 2.

Different types of mechanical stimulation, including compression, shear and tension have also been researched for tissue engineered meniscus. For example, unconfined compression has been applied on meniscus and cartilage to examine their surface layers' functional behavior in Lai and Levenston's research[23]. In this research, meniscus and articular cartilage explants are subjected to unconfined compression(Figure 1.4.4). Digital image correlation(DIC) is used for tracking the samples' 2D deformation. It is found that all cartilage explants showed increased compressive strains in surface layer, while the meniscus samples showed highly heterogeneous strains during compression. The compressed meniscus samples showed 1) high stiffness near surface or 2) comparable stiffness through depth.

Tensile stimulation has also been used, for example, Vanderplog et al[24] argued that tension can be of great significance for injury repairing, especially for tissue engineered scaffolds. Substantial tensile strains can result after implanting a scaffold into a defect site. They introduced a dynamic tensile stimulation(1.0 Hz, 0-10% displacement) into a 3D culture system(Figure 1.4.5) to moderate the matrix synthesis and cytoskeletal organization of bovine articular chondrocytes and meniscal fibrocondrocytes. These experiments revealed that the oscillatory tension inhibited the synthesis of matrix for both cell types. While it obviously increased chondrocytes' proliferation, the same was not true for MFCs. The cell morphology of MFCs turned from rounded shape to a 3D stellate morphology with organized cytoskeletal filaments. These biomechanical and morphological results are of great importance to the cartilage and fibrocartilage tissue repairing strategies.

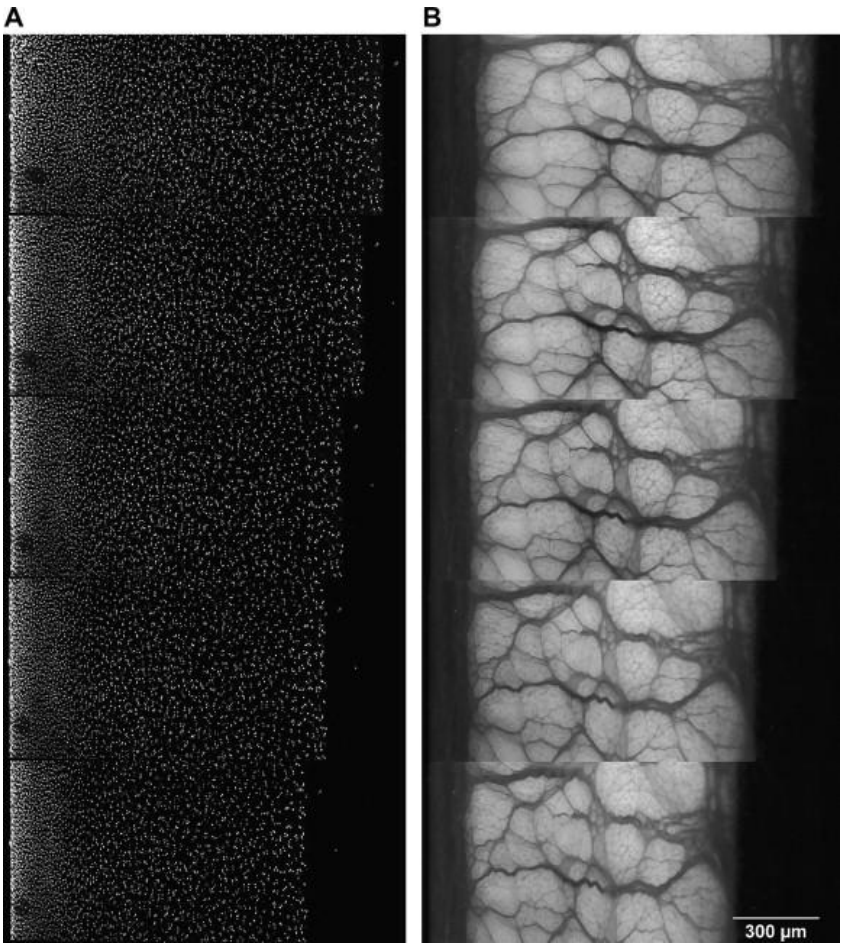

Figure 1.4.4 Fluorescence images of (A) cartilage(cell nuclei) and (B) meniscus (fiber network) samples. Uncompressed, 5%, 10%, 15% and 20% applied strain from top to bottom. From reference 23.

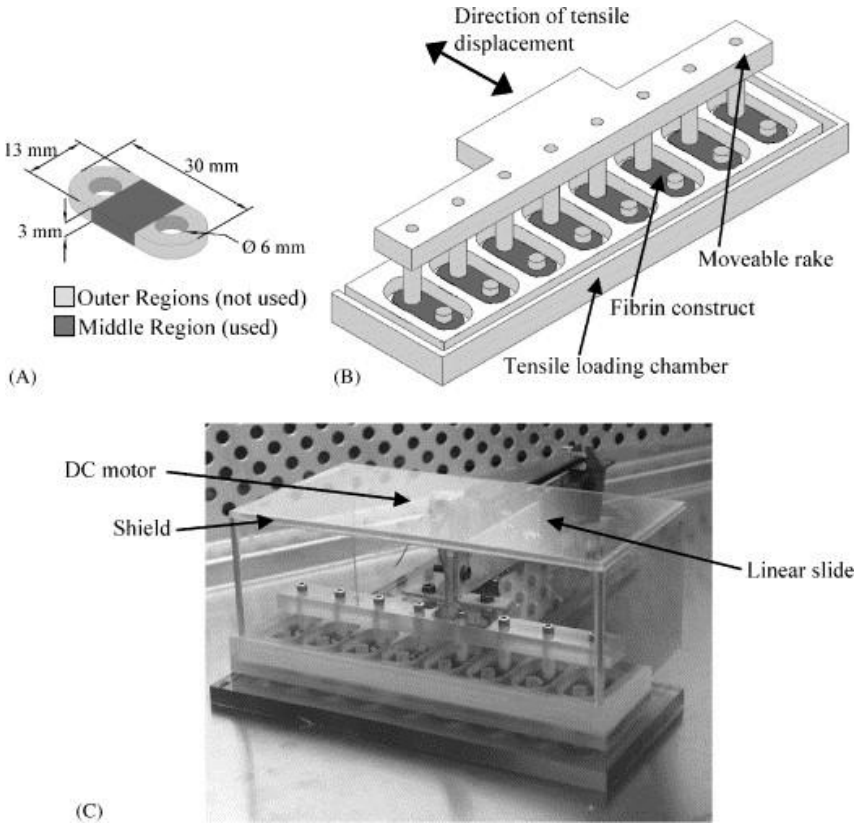

Figure 1.4.5 A. Fibrin construct geometry; B. Tensile loading system; C. Tensile loading system combined with a DC motor for controlling frequency and amplitude. From reference 24.

To figure out how the applied mechanical loading works in the meniscal enthesis, we need to look into the microstructre of the enthesis. Boys et al. demonstrated that the soft tissue-to-bone interface structure is composed of three parts: mobile collagen fiber units, continuous interfacial part, and the local stiffness gradient[25]. In mobile collagen fiber units, the oriented collagen fibers allow for large displacements through fiber sliding. It allows for lateral movement of meniscus without resulting in high strains in the interface region. When it transitions to the disorganized fiber bundles, only small strains are allowed. And then the local stiffness region provides an area of attachment for the disorganized

fiber bundles. Because of this specific construction, strain is concentrated in regions of high fiber sliding and is minimized in the soft-to-bone interface. As such, it provides the extensive mobility in soft tissue while avoids stress concentrations at the interface. For tissue engineered meniscus, it is of great significance to mimic and reproduce the transition from disorganized fiber bundles to oriented fibers in bone-to-soft tissue region.Since the oriented fiber bundle region is of great importance to meniscal movement, we aim to develop a method to introduce more oriented fiber bundles into the soft tissue portion of the constructs.

1.5 Thesis Experimental Design

Inspired by the method of clamping, the idea of introducing mechanical stimulation along the longitudinal direction (stretching) of the TE meniscal enthesis model based on clamped constructs is used in this study. Tensile loading is expected to be created by this method along longitudinal direction in order to stimulate cells and regulate cells' behaviors. To be exact, we expect more organized fiber bundles, especially longitudinal fibers in soft tissue through introducing the stretching stimulation. We also assume that constructs cultured using this method will have a better ability to resist stretching and maintain the firm connective integration at interface. The stretching stimulation will be applied to the clamped constructs for exploration of effect on connective integration of interface. For this purpose, the design of a bioreactor that can provide both clamping and stretching function is required.

1.6 References

1. Diab, M. *Lexicon of Orthopaedic Etymology*. Taylor & Francis (1999).

2. McCorry, M., Mansfield, M. and Bonassar, L. A model system for developing a tissue engineered meniscal enthesis. *Acta Biomater*, 2017. 56, pp. 110-117.

3. Alexander, R., Markes, J. D., Hodax, C. and Ma, B. Meniscus Form and Function. *Clinics in Sports Medicine*, 2020. 39(1), pp. 1-12.

4. "enthesis". Medcyclopaedia. GE. Archived from the original on 2012-02-05.

5. Thomopoulos, S., Birman, V. and Genin, G. (Eds.). *Structural interfaces and attachments in biology.* New York, NY: Springer (2012).

6. Rothrauff, B. B. and Tuan, R. S.. "Cellular therapy in bone-tendon interface regeneration". *Organogenesis*, 2014. 10(1), pp. 13-28. doi:10.4161/org.27404

7. Bedi, A., Kelly, N. H., Baad, M., Fox, A. J. S. and Brophy, R. H. Maher Dynamic contact mechanics of the medial meniscus as a function of radial tear, repair, and partial meniscectomy. *J. Bone Joint Surg. Am*., 2010. 92, pp. 1398-1408.

8. McDermott, I. D. and Amis, A. A. The consequences of meniscectomy. *J. Bone Joint Surg. Br*., 2006. 88, pp. 1549-1556.

9. GBD 2015 Disease and Injury Incidence and Prevalence Collaborators (October 2016). "Global, regional, and national incidence, prevalence, and years lived with disability for 310 diseases and injuries, 1990-2015: a systematic analysis for the Global Burden of Disease Study 2015". *Lancet*. 388 (10053), pp. 1545-1602. doi:10.1016/S0140-6736(16)31678-6. PMC 5055577. PMID 27733282.

10. March, L., Smith, E. U., Hoy, D. G., Cross, M. J., Sanchez-Riera, L., Blyth, F., Buchbinder, R., Vos, T. and Woolf, A. D. "Burden of disability due to musculoskeletal (MSK) disorders". Best Practice & Research. *Clinical Rheumatology*. 2014. 28(3), pp. 353-366. doi:10.1016/j.berh.2014.08.002. PMID 25481420.

11. Hutchinson, I. D., Moran, C. J., Potter, H. G., Warren, R. F. and Rodeo, S. A. Restoration of the meniscus: form and function. *Am. J. Sports Med.*, 2014. 42(4), pp. 987-998.

12. Beynnon, B. D. Meniscal injuries. *DeLee and Drez's Orthopaedic Sports Medicine: Principles and Practice*, 2010. 2, pp. 1596-1623.

13. Ballyns, J. J., Wright, T. M. and Bonassar, L. J. Effect of media mixing on ECM assembly and mechanical properties of anatomically-shaped tissue engineered meniscus. *Biomaterials*, 2010. 31(26), pp. 6756-6763.

14. Ibarra, C., Jannetta, C., Vacanti, C. A., Cao, Y., Kim, T. H., Upton, J. and Vacanti, J. P. Tissue engineered meniscus: a potential new alternative to allogeneic meniscus transplantation. 1997. In *Transplantation proceedings* (Vol. 29, No. 1-2, pp. 986-988). Elsevier.

15. Malvankar, S. M, and Khan, W. S. An overview of the different approaches used in the development of meniscal tissue engineering. *Curr Stem Cell Res Ther*, 2012. 7(2), pp. 157-163.

16. Lee, C., Rodeo, S. and Mao, J. Protein-releasing polymeric scaffolds induce fibrochondrocytic differentiation of endogenous cells for knee meniscus regeneration in sheep. *Sci. Transl. Med.*, 2014. 6(266), pp. 266ra171-266ra171.

17. Szojka, A., Lalh, K., Andrews, S. H. J., Jomha, N. M., Osswald, M., & Adesida, A. B. (2017). Biomimetic 3D printed scaffolds for meniscus tissue engineering. Bioprinting, 8(April), 1 – 7.

18. Villegas, D. F., Hansen, T. A. Liu, D. F. and Haut Donahue, T. L. A quantitative study of the microstructure and biochemistry of the medial meniscal horn attachments. *Ann. Biomed. Eng*., 2008. 36, pp. 123-131.

19. Gao, J. Immunolocalization of types I, II, and X collagen in the tibial insertion sites of the medial meniscus. *Knee Surg. Sports Traumatol. Arthrosc*. 2000. 8, pp. 61-65.

20. Boys, A. J., McCorry, M. C., Rodeo, S., Bonassar, L. J. and Estroff, L. A. Next generation tissue engineering of orthopedic soft tissue-to-bone interfaces. *MRS communications*, 2017. 7(3), pp. 289-308. doi:10.1557/mrc.2017.91. Epub 2017 Oct 3. PMID: 29333332; PMCID: PMC5761353.

21. Walter, B. A., Illien-Jünger, S., Nasser, P. R., Hecht, A. C. and Iatridis, J. C. Development and validation of a bioreactor system for dynamic loading and mechanical characterization of whole human intervertebral discs in organ culture. Journal of Biomechanics, 2014. 47(9), pp. 2095-2101.

22. Manokawinchoke, J., Pavasant, P., Limjeerajarus, C. N., Limjeerajarus, N., Osathanon, T. and Egusa, H. Mechanical loading and the control of stem cell behavior. *Archives of Oral Biology*, 2021. 125(January), 105092.

23. Lai, J. H., & Levenston, M. E. (2010). Meniscus and cartilage exhibit distinct intra-tissue strain distributions under unconfined compression. Osteoarthritis and Cartilage, 18(10), 1291 – 1299.

24. Vanderploeg, E. J., Imler, S. M., Brodkin, K. R., García, A. J., & Levenston, M. E. (2004). Oscillatory tension differentially modulates matrix metabolism and cytoskeletal organization in chondrocytes and fibrochondrocytes. Journal of Biomechanics, 37(12), 1941 – 1952.

25. Boys, A. J., Kunitake, J. A. M. R., Henak, C. R., Cohen, I., Estroff, L. A., & Bonassar, L. J. (2019). Understanding the Stiff-to-Compliant Transition of the Meniscal Attachments by Spatial Correlation of Composition, Structure, and Mechanics. ACS Applied Materials and Interfaces, 11(30), 26559 – 26570.

CHAPTER 2. BIOREACTOR DESIGN FOR CULTURE WITH AXIAL STRETCHING

2.1 Introduction to Bioreactors

2.1.1 Bioreactors' Definition and Functions

As a rapidly developing branch of biomedical engineering, tissue engineering combines the principles of cell biology and engineering, aiming at producing bio-active tissue substitutes that can repair injured tissues or regenerate them. The term bioreactor is used in this thesis to refer to a system or a device that is designed for cell or tissue culture[1]. These devices have been widely developed and used in the fields of tissue engineering and biochemical engineering. For example, Freed[2] used a cell-polymer-bioreactor system for cartilage matrix regeneration and it provides a model system for research in chondrogenesis. Hoerstrup[3] used a pulsatile-flow-bioreactor to provide a biomimetic envrironment *in vitro* for the generation of functional tissue engineered heart valves (TEHV), which showed comparable mechanical properties to native tissues. Bioreactors are not only playing a significant role in cell proliferation and tissue construction, but they are also able to control the pH value, oxygen dissolution, mechanical loading, nutrient supply, removal of metabolites, and so on. These functions provide the most suitable environment for cell growth, differentiation, and proliferation during tissue culture.

2.1.2 Basic Requirements for Bioreactor Design

Here are some basic requirements that bioreactors should meet for cell culture: First, the culture media in bioreactor system should be mixed evenly to avoid gradients of nutrients or pH during cell culture. This feature enables more oxygen and nutrition transfer and accordingly, fuller expression of cell phenotype. Second, the bioreactor design should minimize damage to cells. This involves factors like bioreactor volume, geometry, cell density, growth factor concentration and so on. Third, the environment that bioreactors provide for cells and tissues should be similar to the *in vivo* situation. For example, as has been introduced, the loading environment of meniscus is quite complicated in human knee joints. The bioreactor should be able to mimic the loading environment for long-term culture. All sorts of different tissues and organs have their own specific *in vivo* environment for normal functioning. Accordingly, bioreactor design must be able to meet these specific needs.

2.1.3 Different Types of Bioreactors

There are different types of bioreactors developed and used in tissue engineering for specific functions with respective features. Here are some main types of bioreactors.

2.1.3 (a) Spinner Flask Bioreactor

The working mechanism of a spinner flask bioreactor is usually to use the paddle agitator to get the culture media stirred. In this way, the mass transfer effect can be improved to ensure the uniform distribution of nutrient and oxygen

dissolution. During the tissue culture process, the tissue scaffolds seeded with cells are usually suspended inside the spinner flask bioreactor and immersed in the culture media for culture. Due to the convection effect in the culture media caused by the agitation, the surface of the scaffold is always in a state of exchange with the media, thus increasing the number of cells that can be cultured. The culture media should be periodically replaced to remove the metabolic waste from cells and ensure the concentration of nutrient concentration[4]. Spinner flask bioreactors have simple structures and low cost for usage (Figure 2.1.3.1). They are widely applied in microcarrier cell culture and tissue culture of tissues such as cartilage and skin. However, one of the disadvantages of using this type of bioreactor is that the shear forces caused by stirring may have negative effect on the cells, especially cells which are highly sensitive to the changes of micro-environmental conditions. For example, Richard et al.[5] found that the spinner flask bioreactor they used during research caused the alteration of cell's homeostasis. Compared with static planar culture, this bioreactor resulted in smaller size of cells and higher level of reactive oxidative species (ROS), indicating that changes of micro-environment in bioreactor can have potential physiological alterations to human mesenchymal stem cells (hMSCs).

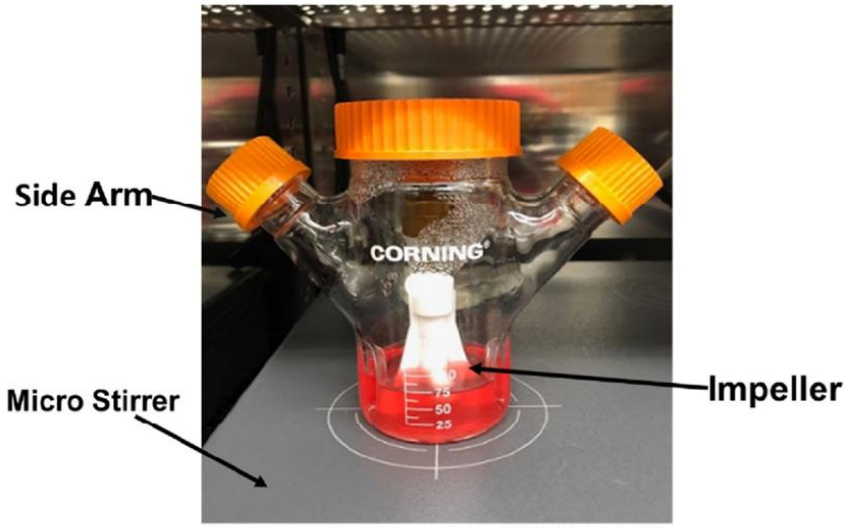

Figure 2.1.3.1. Spinner flask bioreactor and impeller for human mesenchymal cell (hMSC) expansition. From reference 5.

2.1.3(b) Rotating-wall Vessel Bioreactor

The rotating-wall vessel bioreactor is one of the most widely used bioreactor in tissue engineering field, usually for the cell culture of cardiovascular and cartilage tissues. It uses a motor to drive a belt and rotate the culture vessel which has a cylindrical shape along the horizontal or vertical axis. Meanwhile, the culture media and tissue mass also rotate along the axis under the driving of the bioreactor[6,7]. Compared with spinner flask bioreactor, wall-vessel bioreactors can provide micro-environment with much lower shear for culture. Gas exchange was carried out through the gas-liquid two-phase interface, and the sterile syringe is used to replace the liquid to supplement the nutrients. One of the advantages of this bioreactor is the centrifugal force created by the rotation can be adjusted through changing the rotating speed of the bioreactor to balance the gravity of tissue in culture. In this case, the tissue can be suspended in the media during the culture

process. This feature avoids direct friction or collision between tissue and bioreactor wall and creates an environment for 3D dynamic culture[8,9,10]. Tyler[11] has reported the bio-process of culturing retinal organoids from mouse pluripotent stem cells using the wall-rotating vessel bioreactor(Figure 2.1.3.2). Compared with static culture, it indicates that the dynamic culture in this bioreactor helps accelerate and improve the growth and differentiation of cultured tissue.

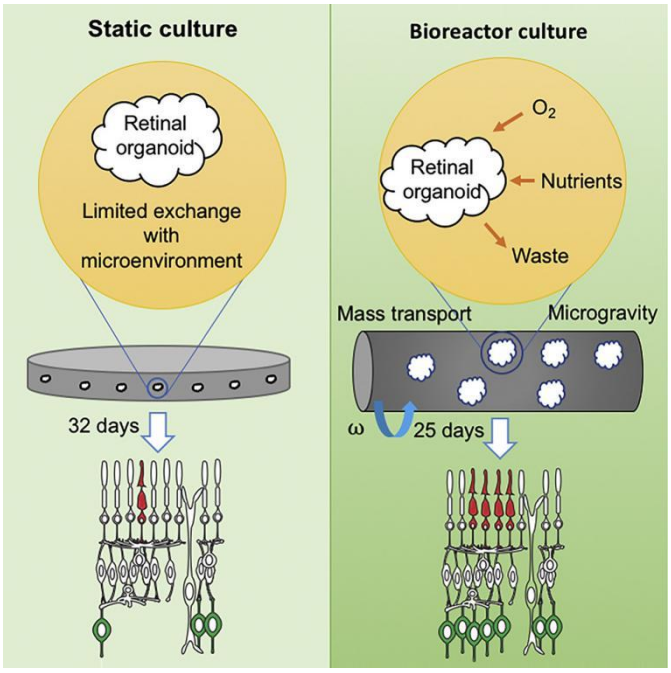

Figure 2.1.3.2. Schematic diagrams of comparison between static culture (left) and bioreactor culture (right) in wall-rotating vessel. From reference 11.

2.1.3(c) Bioreactors with mechanical stimulation

The loading environment during culture is of great significance to the cultured tissue. Cells are subjected to varieties of different mechanical stimulation *in vivo*, which has a great impact on the structure, morphology and functions of tissues[12]. The bioreactors with mechanical force stimulation are designed to introduce mechanical stimuli during culture process and mimic the *in vivo* loading

environment of tissues. For instance, a bioreactor with tunable stretching function for the culture of tissue engineered cardiac construct was designed and tested by Giovanni (Figure 2.1.3.3)[13]. In this research the bioreactor provides tunable mechanical stretching function for biomimetic dynamic culture and it proves that the cyclic stretching stimulation shows effectiveness on cardiac construct maturation.

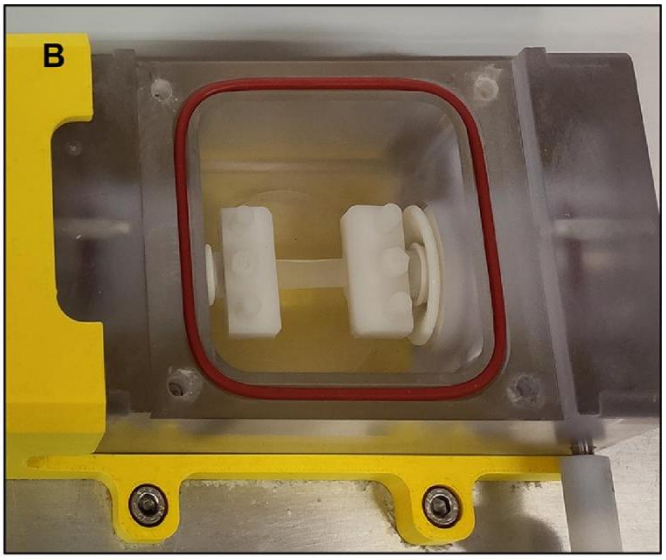

Figure 2.1.3.3. Top view of the culture chamber with clamping accessories of the stretching bioreactor. From reference 13.

It is well established that applying mechanical stimulation to cultured tissues guides the differential formation of tissues. For example, Huey et al. applied tensile and compressive loading to an anatomically-shaped meniscus structure and this stimulation improved the mechanical and biochemical properties of the tissue[14]. In this work, significant additive increases were obtained in compressive instantaneous (3-fold) and relaxation moduli (2-fold), tensile moduli in the circumferential (4-fold) and radial (6-fold) directions. They used these

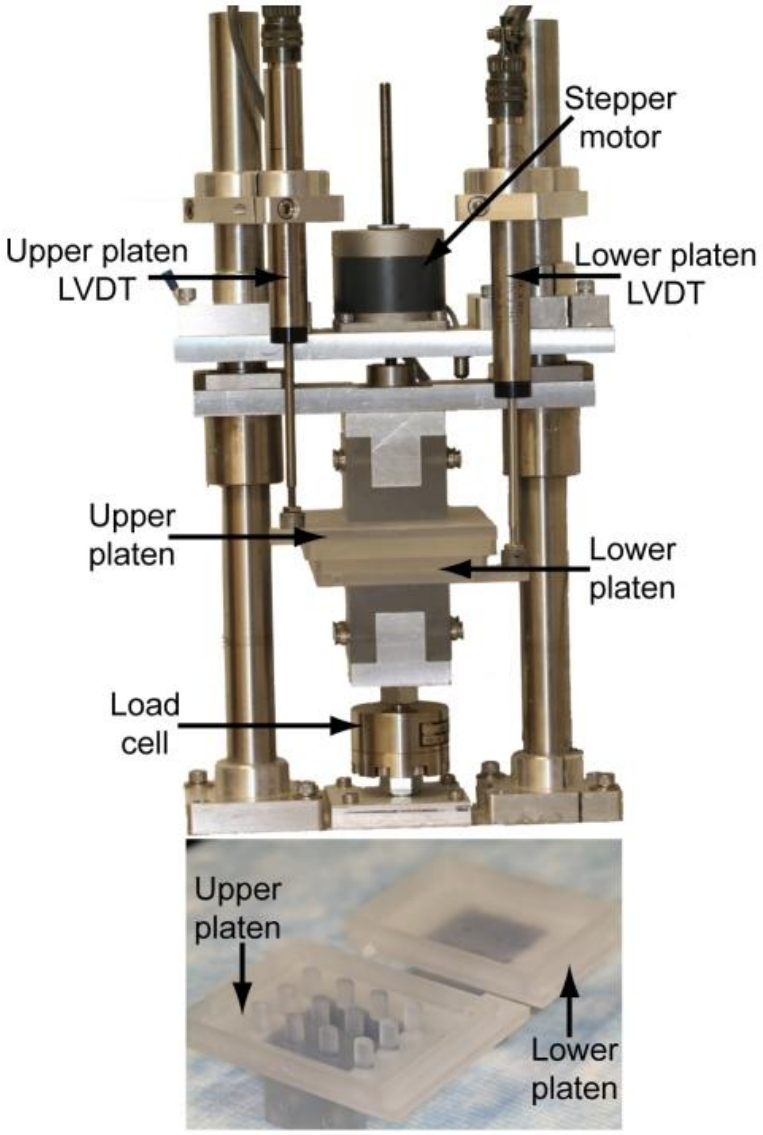

Figure 2.1.3.4 Mechanical stimulation apparatus used during culture (upper) and rapid prototyped stimulation platens (lower). From reference 14.

stimulations to mimic the native loading conditions in human knees. Their bioreactor has a curved-wedge profile to translate compressive loading to circumferential loading. It also has a ring structure to match the curvature of the meniscus and to allow the generation of forces within the constructs. The combined tension and compressive stimulations were applied simultaneously onto

the meniscal constructs for 5 days during culture through a stimulation apparatus (Figure 2.1.3.4) with a 10% axial strain and 1 Hz frequency. Within the 5 days, the constructs were subjected to the mechanical stimulation for 1 hr everyday with 1-minute dynamic stimulation and 1-minute rest, in total 30 cycles. This was the first study to apply combined compression and tension mechanical stimulation of meniscal constructs. It proved that this stimulation can increase the biochemical and biomechanical properties of tissue engineered meniscus.

Another example is the study of Puetzer[15] et al. In this research they designed a bioreactor (Figure 2.1.3.5) that allowed anchoring the tissue engineered menisci at horn attachments and provided compressive loading with a matched condyle loading platen. This bioreactor further mimicked the complex loading environment of native meniscus. It applies tensile and compressive loading in meniscus according to the anatomic location of native tissue. They anchored the meniscus constructs onto the bioreactor at their horns and used 3D printed condyle-shaped platens to apply the mechanical stimulation. It turned out that the mechanical loading improved and accelerated the development of meniscal organization and tensile anisotropy, resulting in more native-like tissue. The loaded menisci showed significantly higher equilibrium and tensile moduli compared with the static samples. The circumferential and radial tensile moduli were also improved after loading. For collagen organization, loaded menisci accelerated the circumferential alignment, growth of collagen fibers and developing of radial

morphologies. The mechanically-loaded menisci developed more heterogeneous tissue organization and composition compared with static clamped samples.

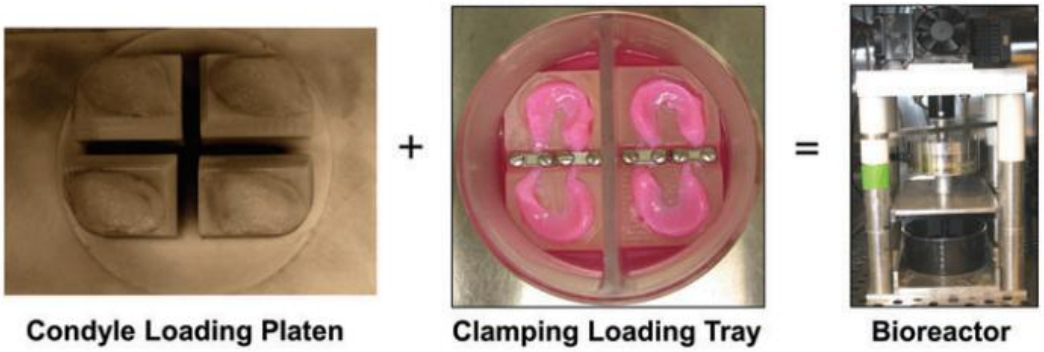

Figure 2.1.3.5 Loading bioreactor composed of (1) condyle loading platen which is generated from ovine MRI and (2) clamping loading tray which mimics native horn attachment. From reference 15.

2.2 Design Requirements

In addition to the most basic bioreactor designing requirements mentioned in the previous section, the bioreactor design in this thesis should also meet these requirements for the realization of stretching function during construct culture as follow: (1) Mechanical stability. The bioreactor should be mechanically stable enough to withstand the forces created during the culture process, especially during clamping and stretching, without being damaged. (2) Chemical stability. Given that the bioreactor needs to be immersed in the culture media for a long time, it needs to be chemically stable to avoid the introduction of any chemicals that could adversely affect the cultured tissue. (3) Sterility. The whole culture process needs to be carried out in a sterile environment. The bioreactor needs to consider

long-term protection against contamination in overall design, including stretching operation, thorough cleaning of the bioreactor and any other aspects. (4) Accuracy and repeatability. Since the stretching function involves the measurement of the stretching length, the stretching function of the bioreactor is required to be stable and repeatable, and the measurement accuracy should be as high as possible to minimize the stretching length error caused by design problems. (5) Volume restrictions. The culture will be carried out in a cylindrical glass container with the 100 mm diameter and 50 mm height. The whole bioreactor will be limited in this volume, including changes in space after stretching. (6) Media usage. From the economic point of view, the volume of culture medium used should be as small as possible on the premise of meeting the culture requirements.

2.3 Stretching Bioreactor Design

In order to achieve the function of stretching the meniscal enthesis constructs during the culture process, a specific bioreactor should be designed and produced. All of the bioreactor design requirements mentioned above need to be considered in a comprehensive manner. The initial concept of the stretching model is based on the polysulfone mold bioreactor used in previous research on clamping effect(Figure 1.4.2. A) [16.] In the ideal stretching bioreactor, it is composed of two part: the movable part (slide) and the fixed part (base). Meniscal enthesis constructs will be fixed onto the bioreactor, stretching across the slide and the base (Figure 2.3.1). A driving system will be used to drive the slide out in realization of

stretching the constructs. Rapid 3D printing technique with polylactic acid (PLA) material will be used for the design and producing work of the bioreactor.

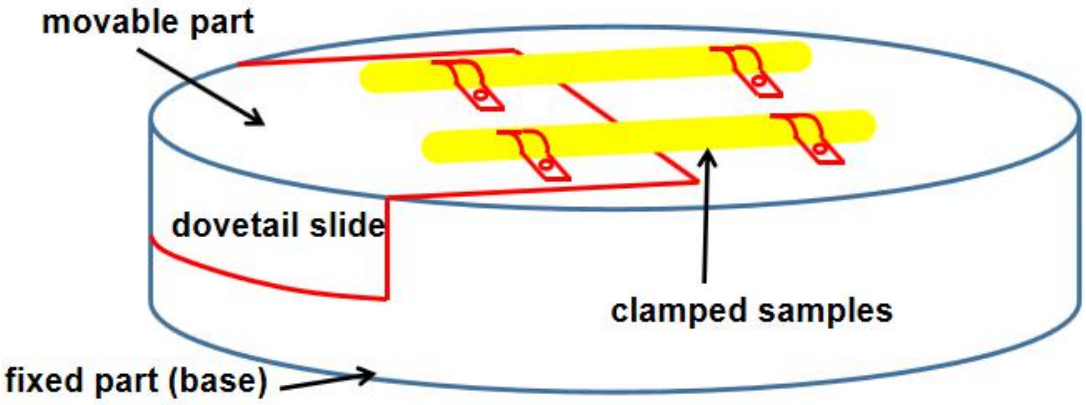

Figure 2.3.1. Schematic diagram of the main components of bioreactor design.

2.3.1 Different Generations of Bioreactor Design

2.3.1(a) Micro-meter Head Driving System on the Top of Bioreactor

The first version of my bioreactor design uses a micro-meter head driving system on the top. This system is composed of three main components: a tab fixed on the slide, a bracket fixed on the base and a micro-meter head used as the driving force source (Figure 2.3.2). The micro-meter head is fixed onto the base by bracket and placed horizontally above the bioreactor. Chambers are designed to make space for two meniscal enthesis constructs on each bioreactor and screw holes are made for clamping at bony ends. For stretching, we will rotate the micrometer-head and it will reach out to the tab. The slide will then be pushed out of the base if we continue rotating the micro-meter head. In this case the stretching function is realized. The stretching length can be read out through the scales on micro-meter head. A locking screw structure is designed on the side of base. When the slide reaches the specific position, a screw will be rotated into the screw hole to

get the slide locked in avoid of any disturbance or slippage. Although the working principle is simple and the bioreactor is easy to operate manually, limitations still exist. Direct contact with culture media will be involved during manual operation since the whole bioreactor will be immersed in media during culture. Due to the limited volume of container, it is inconvenient to reset the screw from the side after each stretching.

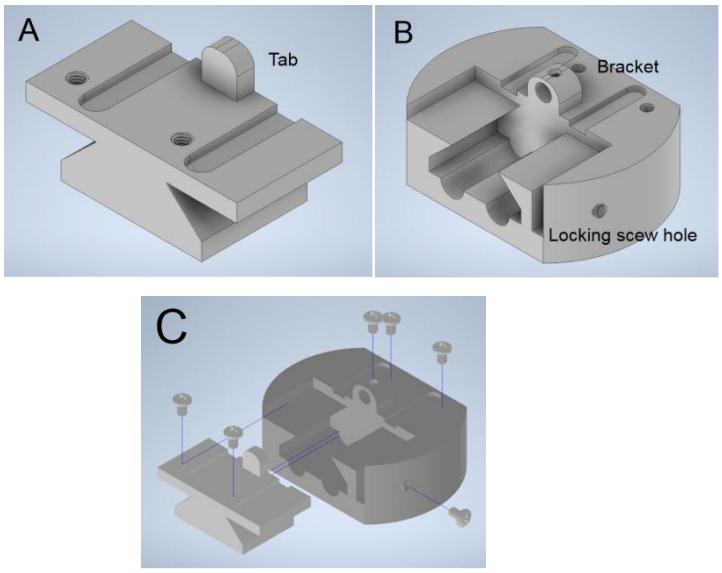

Figure 2.3.2. 3D model images of micro-meter head driven bioreactor. A: slide with tab structure; B: base with bracket and screw locking structure; C: assembly diagram with screws.

2.3.1(b) Micro-meter Head Driving System beneath Container

Based on another micro-meter head, which is already attached to the slide and base, we came up with a new bioreactor. In this design, the driving system is underneath the culture container. Screws will be used to connect the whole micrometer head device with the constructs inside the container. In this case, direct contact with culture media will be avoided since the driving system is outside the

container(Supplemental Figure S3). We planned to drill holes in the bottom of the glass container to complete the connection, however, sealing the container turned out to be a much more difficult problem to solve. Considering the difficulty and feasibility of implementation, this version of design was eventually abandoned.

2.3.1(c) Gear-rack Driving System

A new mechanism of gear-rack driving is used in this version of bioreactor (Figure 2.3.3). A gear is designed to be half buried into the base body and engage with the rack inside the bioreactor. The slide is printed out with the rack as a whole. Manual operation will rotate the gear, then drive the rack outwards in order to drive the slide out. Designs of chambers and screw holes remain unchanged while the whole structure will be produced with PLA material by 3D printing in this version. It reduces the possibility that the introduction of a variety of different materials in the media will have a potential impact on the experiment. For example, metal micrometer head used in version (b) will probably result in rust after long-term culture. However, it does not solve the problem of manual direct contact with culture media. A screw hole locking structure is still needed in this design.

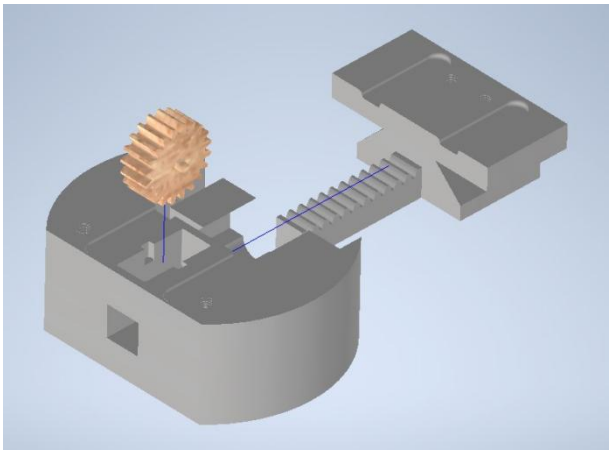

Figure 2.3.3. 3D model diagram of components assembly in gear-rack driving bioreactor.

2.3.1(d) Worm-gear Driving System

In addition to the gear and rack design, we have added a new worm gear structure, which allows us to manually drive the bioreactor in the vertical direction to perform the stretching function (Figure 2.3.4). The change of direction can avoid direct contact with the media by manual operation. For the connection structure between worm and base, fragile snap-lock structure printed with PLA was changed into screw connection. Again, previous designs of the chambers and screw holes for fixation of meniscal enthesis constructs are retained in this version. The other problem of screw locking structure is also solved in this version of design. Due to the self-locking nature of worm-gear structure, no additional locking structure is required to lock the slider at the desired position at any time.

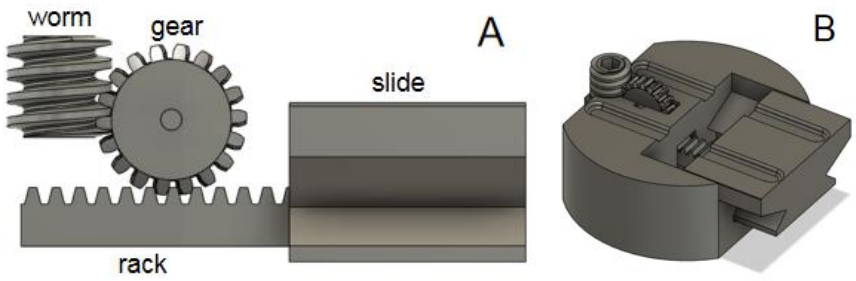

Figure 2.3.4. A: schematic diagram of worm-gear drive system; B: 3D model diagram of worm-gear driven bioreactor

2.3.1(e) Optimization on Worm-gear Driving Bioreactor

In the design of this version, we summed up some details in the testing process of worm-gear driven bioreactor and worked to improve them (Supplemental Figure S4). Firstly, the screw connection structure between worm and base is reinforced to better withstand the drive force during rotation. Secondly, the cross section of the chambers for placing meniscal enthesis constructs was a rectangle, which resulted in twisting problem when fixing the cylindrical constructs.(Supplemental Figure S2) As a result, the tension applied by the bioreactor could not be along the axial direction and thus affected the tensile effect. Therefore we changed the chambers into half-cylindrical ones for better fixation. Thirdly, we adjusted the position of screw holes used for fixing constructs. Lastly, the overall height of the bioreactor was decreased to save the media used from 110 ml to 90 ml for each time of media change in one container.

2.3.2 Features of Current Bioreactor

In this Section, I will discuss the design details, characteristics, advantages, and disadvantages of current bioreactors in use as a summary of the whole design process and to prepare for better bioreactor designs in the future.

The worm-gear structure is a commonly used gear arrangement in mechanics. It has the basic functions of reducing rotation rate or transmitting torque as a gear arrangement. During the meshing between worm and gear, the sliding and rolling actions of worm and wheels are combined together to function[17]. Apart from that, unlike other gear drives, the direction of transmission from input to output in worm-gear structure is irreversible[18], which means it is a one-way path from input to output. The gear can not drive the worm backwards. In this case the slide will be locked at the exact stretching position without subsequent displacement. This is one of the special features of worm-gear structure called 'self-locking' and is one of the main reasons why worm-gear-rack drive system is used in the design. It successfully got us out of the locking structure dilemma.

To be more detailed, the interior of the worm is designed as a hollow structure, and the cross section of the inner hole is regular hexagon (Figure 2.3.5 A). In this case we can use a hexagon wrench to rotate the worm from above the bioreactor rather than directly touching it with our hands. This design greatly reduces the likelihood of infection being introduced. For the connection between worm and base, snap-lock structure was initially designed and tested (Figure 2.3.5 B). It is a locking structure using a catch or a snap with a hook-like end. However,

it turned out that the precision and material strength of the 3D printer we used could not meet the connection requirements (Figure 2.3.5 C, Supplemental Figure S1 A,D). Accordingly, we switched to screw connection structure which is more reliable for connection and detachable compared with snap-lock.

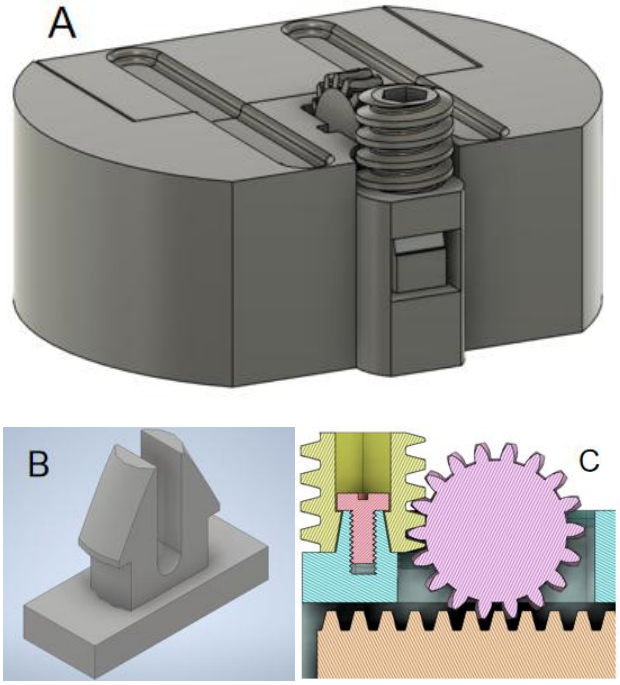

Figure 2.3.5. A: 3D model diagram of worm-gear structure; B: 3D model diagram of snap-lock structure; C: slide profile image of worm-gear-rack inner structure with screw connection.

For stretching function of the bioreactor, the distance the slide is driven outwards does not uniformly increase with the rotation on worm, which theoretically should be. After testing, the complete process from the beginning of rotation to the end is composed of a non-linear stretching process and a linear one, according to the distance measured. This results from the slack between worm and gear. To solve this problem, the slide will be driven out in advance in order to skip

the nonlinear part before meniscal enthesis constructs are fixed onto the bioreactor so the stretching will start from the linear part. For the linear stretching part, the distance that the slide is driven out for every 45° of rotation on worm is 0.423 mm on average (Supplemental Figure S5, Supplemental Table S1).

Limitations of the current bioreactor still exist. PLA material has poor heat resistance and cannot be sterilized by autoclaving. The bioreactor needs to be immersed in 70% ethanol under UV light for 24 hours both before and after culture experiment for sterility instead. Higher resolution in 3D printing is needed in order to achieve higher accuracy in stretching distance and less experimental errors (Supplemental Figure S1 B,C).

2.4 References

1. Popović, M. K. and Pörtner, P. Bioreactors and cultivation systems for cell and tissue culture (2012). Biotechnology. *Encyclopedia of life support systems (EOLSS), Developed under the Auspices of the UNESCO, Eolss Publishers, Oxford, UK. http://www.eolss.net*.

2. Freed, L. E., Hollander, A. P., Martin, I., Barry, J. R., Langer, R. and Vunjak-Novakovic, G. Chondrogenesis in a cell-polymer-bioreactor system. *Experimental Cell Research*, 1998. 240(1), pp. 58-65.

3. Hoerstrup, S. P., Kadner, A., Melnitchouk, S., Trojan, A., Eid, K., Tracy, J., Sodian, R., Visjager, J. F., Kolb, S. A., Grunenfelder, J., Zund, G. and Turina, M. I. Tissue engineering of functional trileaflet heart valves from human marrow stromal cells. Circulation, 2002. 106(13 SUPPL.), pp. 143-150.

4. James, K. H. and Krishna, G. G. Tissue engineering with chondrocytes. *Facial Plastic Surgery*. 2002. 18(1), pp. 59-68.

5. Richard Jeske, Shaquille Lewis, Ang-Chen Tsai, Kevin Sanders, Chang Liu, Xuegang Yuan, Yan Li, Agitation in a microcarrier-based spinner flask bioreactor modulates homeostasis of human mesenchymal stem cells, Biochemical Engineering Journal,Volume 168, 2021, 107947, ISSN 1369-703X.

6. Kleis, S. J. and Schreck, S. A. Viscous pump bioreactor. *Biotechnol. Bioeng*. 1990. 36, pp. 771-777.

7. Muzzio, F. J., Unger, D. R. and Liu, M. Computational and experimental investigation for flow and particle settling in a roller bottle bioreactor. *Biotechnol. Bioeng*. 199. 63(2), pp. 185-196.

8. Begley, C. M. and Kleis, S. J. The fluid dynamic and shear environment in the NASA/J SC rotating-wall perfused-vessel bioreactor. *Biotechnol. Bioeng*. 2000. 70(1), pp. 32-40.

9. Goodwin, T. J., Prewett, T. L. and Wolf, D. A. Reduced shear stress: a major component in the ability of mammalian tissues to form three-dimensional assemblies in simulated microgravity. *J. Cell. Biochem*. 1993. 51, pp. 301-311.

10. Freed, E., Langer, R. and Martin, I. Tissue engineering of cartilage in space. *Proc. Natl. Acad. Sci. USA*. 1997. 94, pp. 13885-13890.

11. DiStefano, T., Chen, H. Y., Panebianco, C., Kaya, K. D., Brooks, M. J., Gieser, L., Morgan, N. Y., Pohida, T. and Swaroop, A. Accelerated and improved differentiation of Retinal Organoids from Pluripotent Stem Cells in Rotating-Wall Vessel Bioreactors. *Stem Cell Reports*, 2018. 10(1), pp. 300-313.

12. Slack, C., Flint, M. H. and Thompson, B. M. The effect of tensional load on isolated embryonic chick tendons in organ culture. *Connect. Tissue Res.* 1984. 12(3-4), pp. 229-247.

13. Putame, G., Gabetti, S., Carbonaro, D., Meglio, F. Di, Romano, V., Sacco, A. M., Belviso, I., Serino, G., Bignardi, C., Morbiducci, U., Castaldo, C. and Massai, D. Compact and tunable stretch bioreactor advancing tissue engineering implementation. Application to engineered cardiac constructs. *Medical Engineering and Physics*, 2020. 84, pp. 1-9.

14. Huey, D. J. and Athanasiou, K. A. Tension-compression loading with chemical stimulation results in additive increases to functional properties of anatomic meniscal constructs. PLoS ONE, 2011. 6, p. e27857.

15. Puetzer, J. L. and Bonassar, L. J. Physiologically distributed loading patterns drive the formation of zonally organized collagen structures in tissue engineered meniscus. Tissue Eng. 2016. A 22, pp. 907-916.

16. McCorry, M. C., Mansfield, M. M., Sha, X., Coppola, D. J., Lee, J. W., & Bonassar, L. J. (2017). A model system for developing a tissue engineered meniscal enthesis. Acta Biomaterialia, 56, 110 – 117.

17. Rybczynski, W. *One good turn: a natural history of the screwdriver and the screw.* London, 2000. p. 139.

18. Gear Nomenclature. Definition of Terms with Symbols. American Gear Manufacturers Association. 2005. ISBN 978-1-55589-846-5. OCLC 65562739. ANSI/AGMA 1012-G05.

CHAPTER 3. EFFECT OF AXIAL STRETCHING ON MENISCAL ENTHESIS CONSTRUCTS

3.1 Introduction

The meniscal enthesis, which is the attachment of the menisci to the underlying bone, plays a very significant role in the mechanical stability and normal biological function of knee joint. For each enthesis (4 in total in one knee joint), it diffuses tensile loading forces transmitted from the meniscus through collagen fibrils[1-7]. In order to function properly, the connective integration of enthesis must be robust and in this case meniscus will be firmly anchored into the underlying bone through these entheses[8,9]. It is known that the integrity of the complex meniscal entheses is highly related to the ability of menisci to prevent osteoarthritis (OA)[10]. Accordingly, for one of the commonly used meniscus repairing methods, meniscal allograft, the preparation work usually includes all-soft tissue fixation, bone plugs or a bone bridge[11], in order to keep the integrity of native meniscal enthesis structure to the maximum extent possible (Figure 3.1.1). It also avoids rebuilding the complex interface between soft tissue and bone[12]. However, there are some limitations to meniscal allograft: lack of donor tissue, mismatched sizes and potential for adverse immune reactions. Autograft is also used as another repairing method that uses part of the patient's native tissue. However, the method involves multiple surgical sites and it is infeasible to harvest autografts from ligament sites.

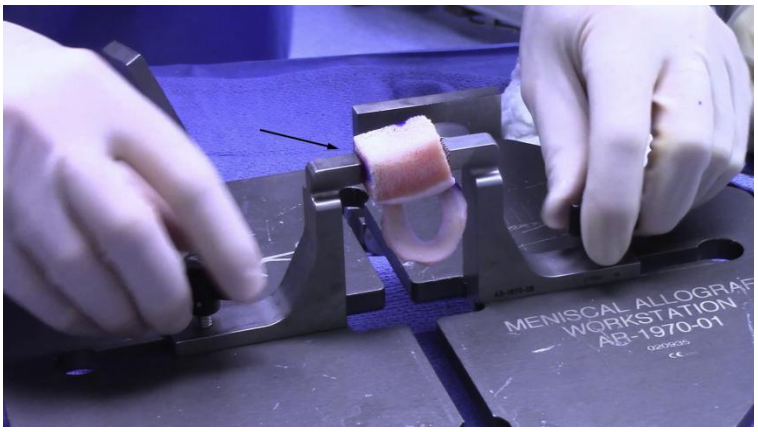

Figure 3.1.1. Preparation of meniscus with dovetail bone bridge during lateral meniscal allograft demonstration video. From reference 11.

As a promising treatment for meniscus repairing, tissue engineered meniscus combines the advantages of both meniscal allograft and autograft. The size and geometry shape of the grafts can be customizable to the patient, and there is no need for donors. Tissue engineered meniscus does not have the native enthesis structure of a meniscus allograft. Therefore, how to implant TE meniscus firmly onto the bone remains a critical problem. However, although much attention and effort has been focused on the construction of scaffolds for meniscus body, little research has been done on the connective integration between TE meniscus to the underlying bone. Native meniscal enthesis is a complex structure due to the the presence of different gradients of cell types, minerals, extracellular molecules and different stress environments[13]. In this study we used a meniscal enthesis construct model to mimic this complex structure as a platform for research and experiments, as has been introduced in former chapter.

In the native meniscal enthesis, there is a dense collagen fiber network structure. These collagen fibers interweave in specific directions and penetrates

into the trabecular bone structure, which plays an important role in facilitating the transmission of compressive and tensile loads[14-17]. In the enthesis zone from soft tissue to bone, the structure transition has promoted the load transfer in the interface region[18-20]. The transferred forces in enthesis, including dynamic tensile, compressive and shear loading, provide the loading environment for cells during culture which transfers mechanical stimulation signals to cells to guide matrix production and remodeling. It is known that disorganized fiber bundles can be resulted from the lack of loading environment during culture[20]. Accordingly, it is of great significance to design proper stimulation during tissue culture.

In the current research, we are aiming to explore the effect of axial stretching stimulation to a meniscal enthesis construct model, which mimics the native meniscal enthesis structure during culture, using a specific bioreactor we designed and produced with 3D printing technique. The native meniscal enthesis is subjected to a very complex loading environment. As part of the complex mechanical loading of the knee, tensile force is designed to be applied onto the clamped meniscal enthesis constructs by stretching during culture for mimicking the native environment in knee joints.We hypothesize that tensile loading will drive the formation of more organized collagen fiber bundles, especially longitudinal fibers and improved mechanical properties for better connective integration between soft tissue and bone.

3.2 Methods

3.2.1 Bone Plugs Extraction

The bone plugs used in this study were prepared according to published methods[21]. Briefly, they were extracted from the distal femurs of 1~3-day-old bovids (Gold Medal Packing Inc.) using an electric drill with a 6 mm coring bit. During dissection process, excess tissue around the head and neck of the femur was removed to expose the surface of the trabecular bone, from which bone plugs were extracted. After drilling out 15 mm long cylindrical bone plugs, a stream of high velocity deionized water was used to rinse out residual blood, marrow and debris from the pore space and keep the white trabecular bone structure. Then bone plugs were washed for 1 hour in PBS with 0.1% (wt/vol) ethylenediaminetetraacetic acid (EDTA) at room temperature. After that, sequential washes in hypotonic buffer (10 mM Trizma base in 100 mL DI water, 0.1 w/v% EDTA) were applied for 1 hour each and at least for three times. Then bone plugs were placed at 4℃ for at least 24 hours. Next, detergent of 10 mM Trizma base with 0.5 w/v% was used for washing bone plugs for at least 3 hours. Again, left at room temperature for 24 hours. Finally, the bone plugs were washed using PBS with antibiotics at least seven times until no bubbles exist.

3.2.2 Rat Tail Collagen Extraction

For the collagen used in this study, it was extracted from rat tail (Pel-Freez Biologicals, Rogers, AZ). The rat tails were immersed in 70% ethanol for 10-20 minutes for thawing. Then the skin of rat tail was cut and peeled off. Then the rat

tail tendon was extracted by holding the end of rat tail and grabbing, bending, twisting, and then pulling at the tips. After being extracted and collected into ethanol, rat tail tendons were dried and then placed into 0.1% acetic acid at 150 mL/gram of tendon. Then the collagen were solubilized for at least 48 hours at 4℃. After that, the collagen solution was placed into 50 mL conical tubes and perfectly balanced in preparation for spinning down. After 15000 rpm for 45 minutes at 4℃, collect the clear supernatant. The supernatant was frozen under -80℃ for 30 minutes and lyophilized for 48 hours. Finally, the collagen product was weighed and reconstituted in 0.1% acetic acid solution. The concentration of the collagen in this study is 30 mg/mL.

3.2.3 FCC Extraction

Fibrochondrocytes (FCC) were extracted from menisci of 1~3-day-old bovids in the knee joints[22]. Menisci were chopped up into 1-2 mm cubes after being dissected from the joint in sterile environment. After that, cubes were placed into PBS with ABAM (Antibiotic Antimycotic Solution, Mediatch, Inc.) and washed for three times and incubated for 30 minutes after the third washing. Then cubes were added into 0.3% collagenase (Worthington Biochemical Corporation, Lakewood, NJ) solution with 1% ABAM for 18 hours of digestion in 37℃ incubator with spinning. Then, the digested tissue were pipetted into 100 μm cell strainers on conical tubes to isolate FCCs. After spinning down the balanced conical tubes at 2500 rpm for 12 minutes, the supernatant was aspirated and cell pellet was dispersed with PBS with 1% ABAM. Conical tubes were used for

centrifuging at 1000 rpm for nine minutes. Then this procedure was repeated. Cell concentrations were adjusted to 150*10^6 cells/mL in media for construct generation.

3.2.4 Construct Generation

As has been introduced, the meniscal enthesis construct is composed of bone zone, collagen zone, and the interface between them[21]. The construct is generated from decellularized bone plugs, type I collagen, and fibrochondrocytes prepared in the former sections. Briefly, marks were made onto Tygon® tubing to divide zones for collagen and bones. Decellularized bone plugs were placed into the tube at both ends and binder clips were used in avoid of bone plugs moving backwards. Holes were cut out at both ends for air flowing during collagen injection and in the center of bone zone for injection. Prepared collagen was mixed with working solution(1 N NaOH, 1x PBS and 10x PBS) and isolated FCCs with media in order to achieve the final collagen mixture with a neutral 7.0 pH, a concentration of 20 mg/mL collagen and 25*10^6 cells/mL. After that the mixture was immediately injected into the central hole and constructs are placed into an incubator under 37℃ for 50 minutes for gelation. After gelation process, constructs were removed from the tube into petri dish with meniscus media and placed in incubator overnight to equilibrate. Finally, constructs were clamped onto polysulfone molds with clamps and screws without stretching as control groups, and onto bioreactors with stretching as experimental groups. Both groups were cultured for the same time periods (2 weeks, 4 weeks). For 2 weeks' culture, all

samples (2 control, 2 experimental) were processed for histology analysis and for 4 weeks' culture, one control and four experimental samples went for tensile testing. All samples were processed for histology analysis.

3.2.5 Culture Experiments

For the 2-week culture experiment, meniscal enthesis constructs were fixed onto polysulfone molds without stretching stimulation, which was set as the control group. And the experimental group constructs were fixed onto stretching bioreactors with axial stretching stimulation. The stretching rate was 2% of initial collagen length (45° rotation on worm) for every 3 days (5 times of stretching in total). Samples from both groups were generated with same decellularized bone plugs and collagen with FCCs under same conditions. The initial length of collagen is 20 mm (Table 3.2.1). After culture, all samples from both groups were processed for Picrosirius red staining and Masson's trichrome staining.

Table 3.2.1. 2-week culture experiment set

	Control Group	Experimental Group
Control	Fixed culture without stretching	Fixed culture with stretching
Samples	20mm collagen with FCCs + decellularized bone plugs	
Reactors	Polysulfone molds	PLA Bioreactors
Distance	-	10% (2mm)
Rate	-	0.4mm(2%) every 3 days
Culture time	14 days	

For the 4-week culture experiment, apart from the culture time change, the stretching distance was changed to 8% of initial length of collagen (1.6 mm). And the stretching rate was changed from 2% every 3 days to 2% every 6 days and constructs will be in total stretched four times. The other parameters remained unchanged (Table 3.2.2). After culture, collagen length of constructs was measured from both groups. Five control group samples and four experimental samples underwent tensile testing. One control group sample and six experimental group samples underwent histology analysis with Picrosirius red staining and Masson's trichrom staining. The images of constructs at different time points are listed in Supplemental Figure S6.

Table 3.2.2. 4-week culture experiment set

	Control Group	Experimental Group
Control	Fixed culture without stretching	Fixed culture with stretching
Samples	20 mm collagen with FCCs + decellularized bone plugs	
Reactors	Polysulfone molds	PLA Bioreactors
Distance	-	8% (1.6 mm)
Rate	-	0.4 mm (2%) every 6 days
Culture time	28 days	

3.2.6 Histology Analysis

When the culture experiments of constructs were complete, samples were placed into 10% buffered formalin to fix them for 48 hours. After fixing, formalin was washed off with ethanol and constructs were longitudinally cut in half to get

the inner structure of meniscal enthesis constructs exposed. Slides of sections were used for Picrosirius red and Masson's trichrome staining. For the Picrosirius red staining slides, they were viewed under brightfield and polarized light with a Nikon Eclipse TE2000-S microscope. The images were taken through a SPOT RT camera.

3.2.7 Tensile Testing

The 4-week-cultured meniscal enthesis constructs went through tensile testing for analysis of mechanical properties. The tensile testing used in this research is based on published method[23]. During the testing process, constructs were clamped at both bony ends and vertically fixed onto the testing system (ElectroForce 5500 System, Bose, Eden Prairie, MN). A rate of 1.5 mm/sec was applied onto the constructs until its failure. For mechanical property analysis, several quantities were calculated as follow: The ultimate load (UL) was the maximum load that the construct can withstand during testing process. The ultimate tensile stress (UTS) was the maximum stress the construct can withstand, and it is when the construct begins to fail. The tensile modulus is the slope of the linear elastic part of stress-strain curve. The toughness is the total area under the stress-strain curve. At the onset and the end of failure, the strain values were also recorded and analyzed.

3.2.8 Statistics

All the data points in this study are graphed in the form of mean ± SD. Data from tensile testing are analyzed with t-testing. Significant difference is determined with $p<0.05$ and difference existence is determined with $0.05<p<0.1$.

3.3 Results

3.3.1 Meniscal Enthesis Constructs After Culture

The meniscal enthesis constructs were generated and cultured on Polysulfone molds (control groups) and stretching bioreactors (experimental groups). The culture time for two experiments were respectively 2 weeks and 4 weeks. Following the same generation method, the bone region and collagen region were obviously recognizable from both control and experimental groups. The collagen penetrated into the trabecular bone plugs and formed the interface region between bone and collagen. After culture, constructs from both groups were stiff enough to withstand conventional physical handling without fracture. In the 2-week culture experiment, observable necking phenomenon was found in samples from experimental group compared with control group samples (Figure 3.3.1.1). While in 4-week culture experiment, there is no observable necking phenomenon in both groups (Figure 3.3.1.2). The length data of constructs after culture is: 19.03 mm ± 0.05 mm for control group; 21.67 mm ± 0.19 mm for experimental group (Figure 3.3.1.3). On average the collagen length was elongated by 8.35% after stretching.

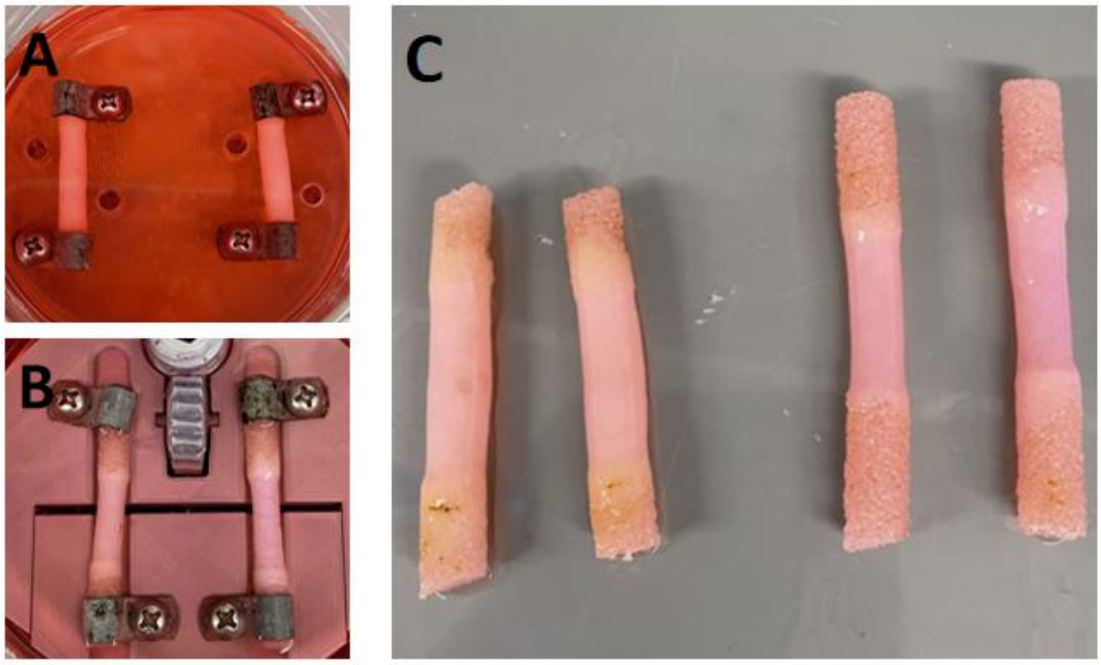

Figure 3.3.1.1. Images of 2-week cultured meniscal enthesis constructs. A: meniscal enthesis constructs on polysulfone mold without stretching; B: meniscal enthesis constructs on bioreactor with stretching; C: comparison between constructs from both groups. Left 2: control group, collagen length:~20mm; Right 2: experimental group, collagen length:~22mm.

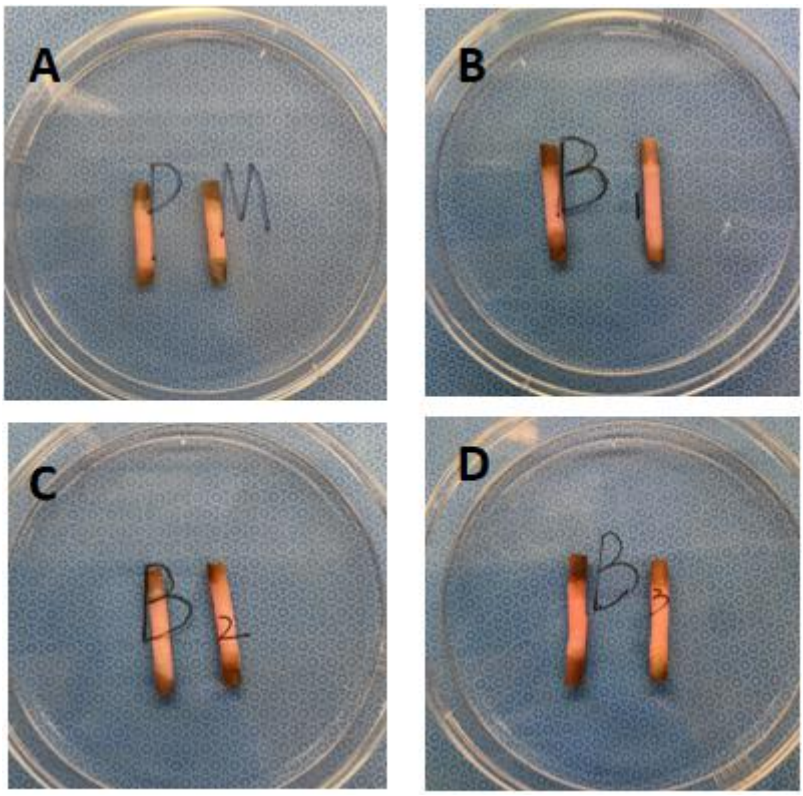

Figure 3.3.1.2. Images of 4-week cultured meniscal enthesis constructs. A: control group samples, collagen length: ~19.03mm; B, C, D: experimental group samples, collagen length: ~21.67mm.

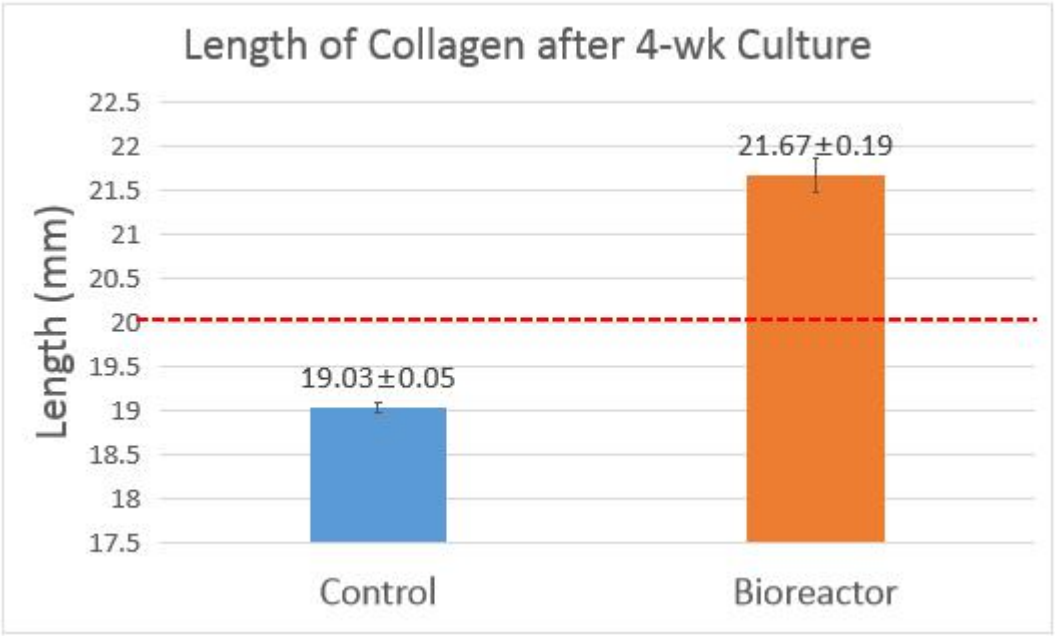

Figure 3.3.1.3. Histogram of collagen length after 4-week culture. Red dotted line shows the initial collagen length of 20 mm.

3.3.2 Histology Analysis

Differences of collagen density can be found by comparing brightfield images of Picrosirius red staining slides at interface region between unstretched constructs and stretched constructs after 2 weeks of culture (Figure 3.3.2.1). The unstretched constructs show higher collagen density at interface compared to stretched constructs. There was obvious banded gap space between bone region and collagen region in stretched constructs, which can be seen as sign of partial failure phenomenon at interface region during stretching process.

Similar features also appear in the Picrosirius red staining slides of 4-week cultured meniscal enthesis constructs. The unstretched construct (Figure 3.3.2.2 A) showed higher density of collagen and less defects at interface and collagen region than the stretched constructs (Figure 3.3.2.2 B,C). Even without observable

necking phenomenon, the 4-week stretched constructs still showed areas of gap space in collagen with more defects.

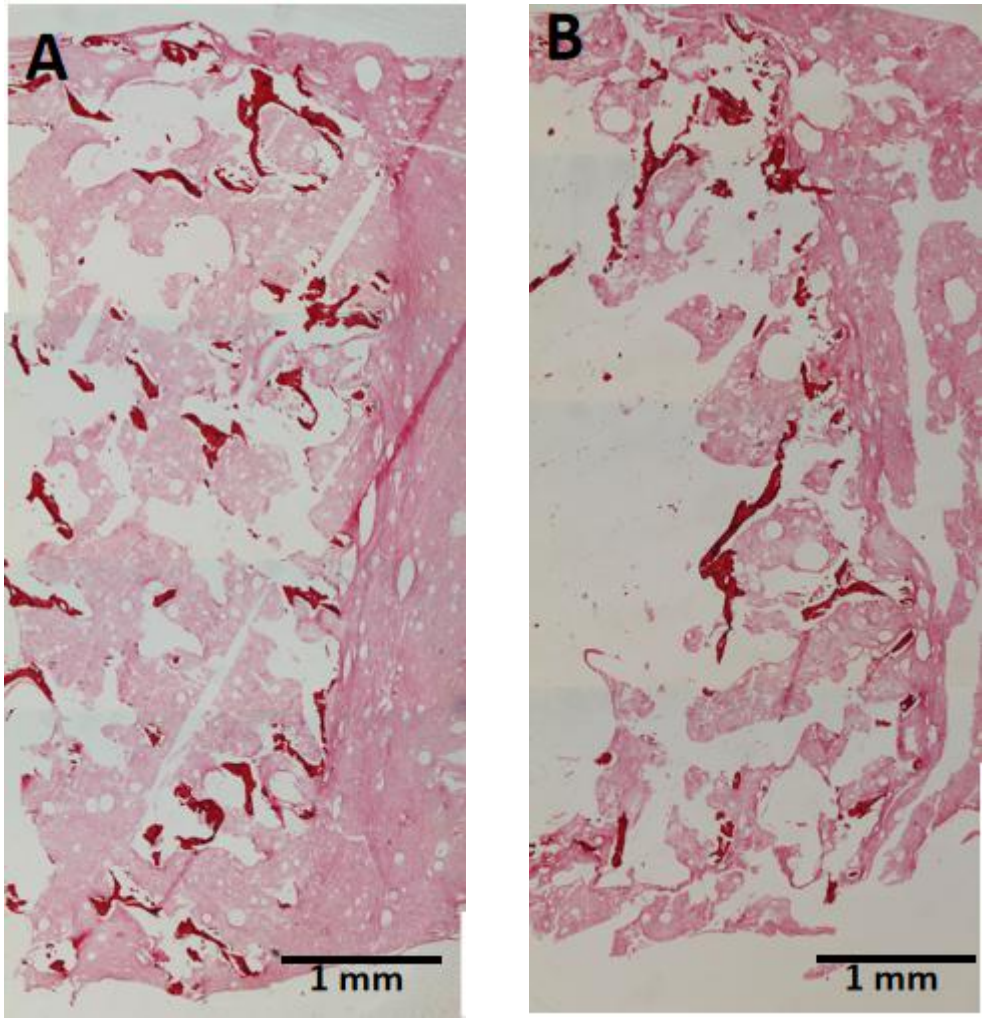

Figure 3.3.2.1. Brightfield images of Picrosirius red staining slides at interface region of: A. unstretched construct; B. stretched construct. Bone region is on the left side.

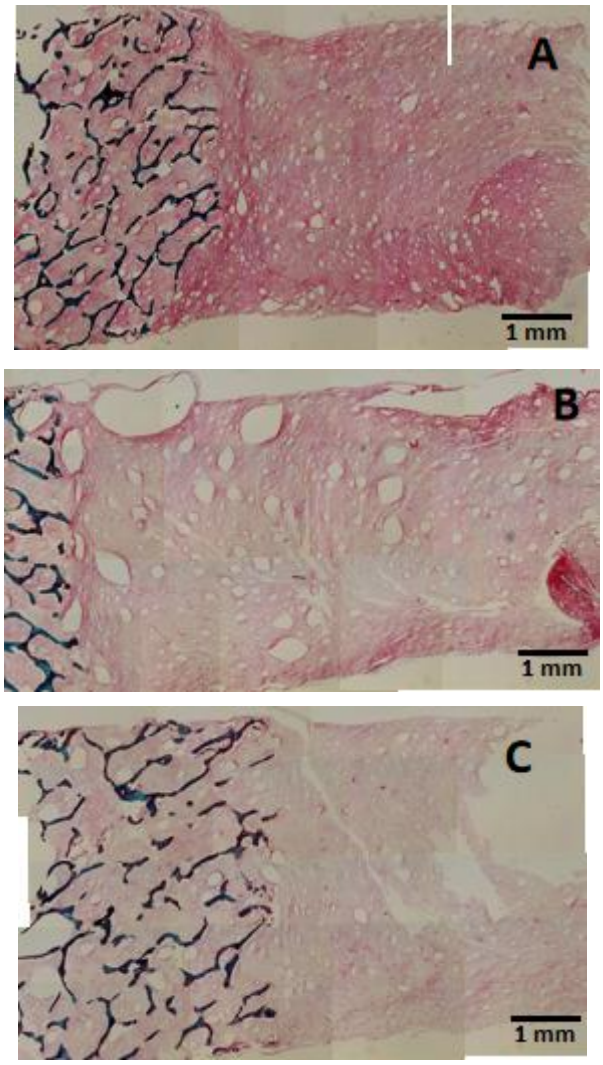

Figure 3.3.2.2. Brightfield images of Picrosirius red staining slides of 4-week cultured meniscal enthesis constructs. A: control group sample; B,C: experimental group samples. Bone region on the left side.

Similarities of fiber orientations were observed at the interface region from polarized light images of unstretched and stretched constructs. For both groups, the collagen fiber orientation is mainly parallel to the edge of the interface, which is along the radial direction. While it shows a trend to turn to longitudinal direction as the fiber bundles extend to the collagen region (Figure 3.3.2.3). This phenomenon was observed both in control groups and experimental groups.

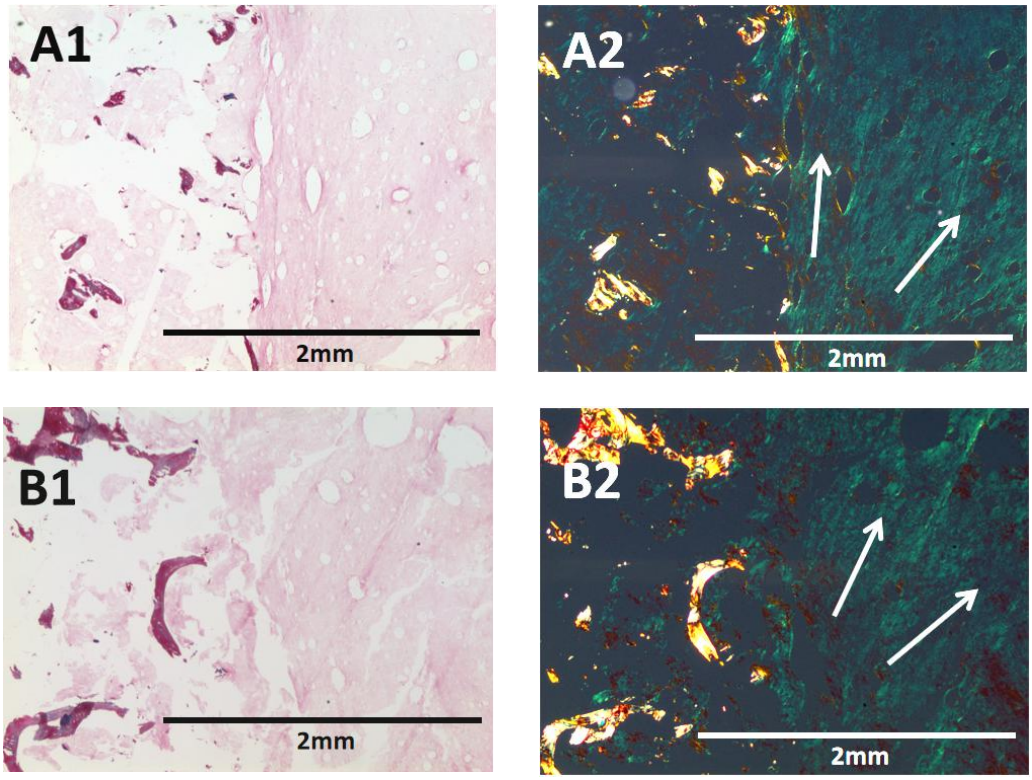

Figure 3.3.2.3. Picrosirius red staining slides of (A) unstretched construct and (B) stretched construct at interface region(2-week culture). A1,B1: Light field images; A2,B2: Polarized light images. White arrows show the main orientation of fiber bundles.

After 4 weeks of culture, there are differences of collagen fiber organization between unstretched constructs and stretched constructs (Figure 3.3.2.4). In unstretched samples, the fiber orientation showed similar pattern as it was in the 2-week culture experiment: fibers are mainly along the radial direction at interface and turn to longitudinal direction in collagen region. While in stretched constructs, large areas of fibers along longitudinal direction were observed at

collagen region, especially at outer edge of collagen region. Meanwhile, less radial fiber orientation was found in stretched constructs compared with unstretched constructs. There were more defects in the collagen part of stretched constructs (Supplemental Figure S7).

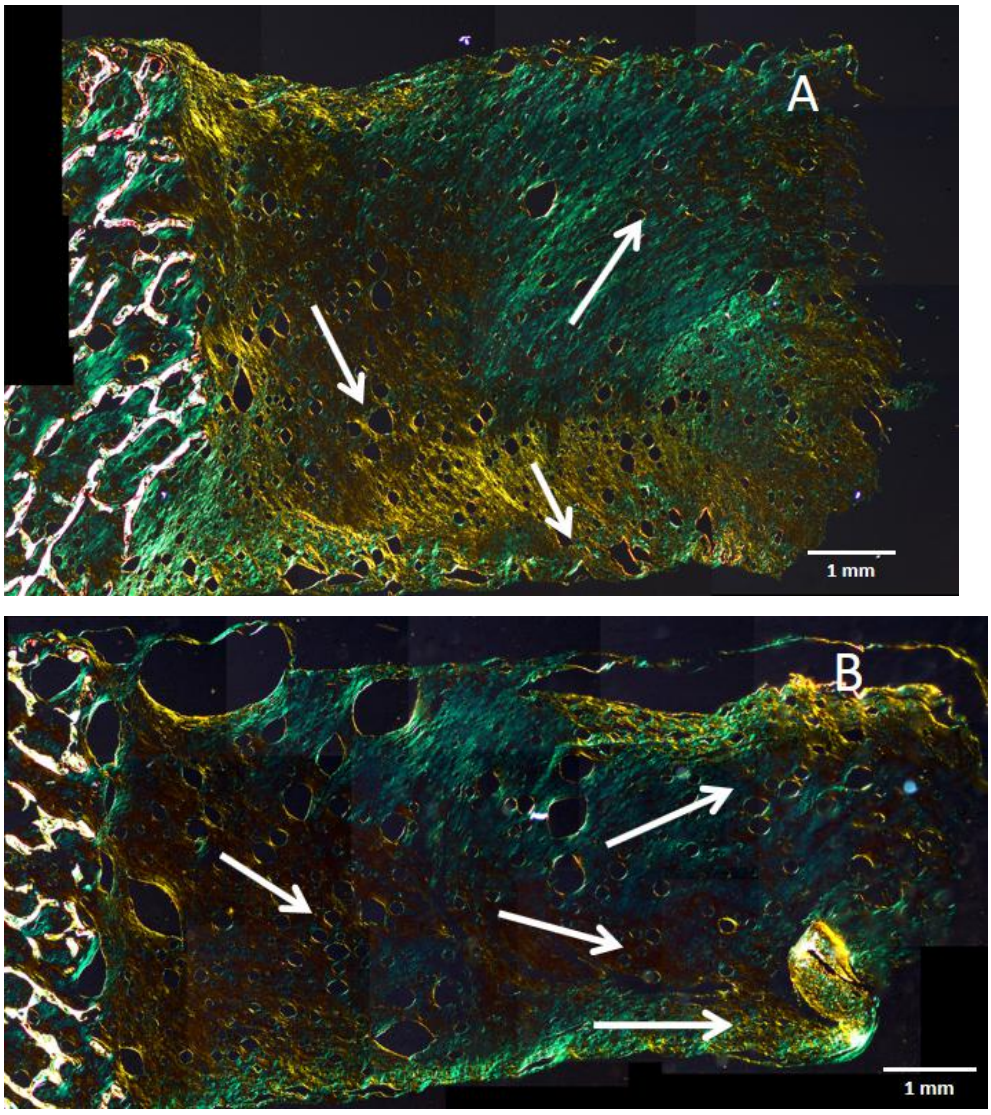

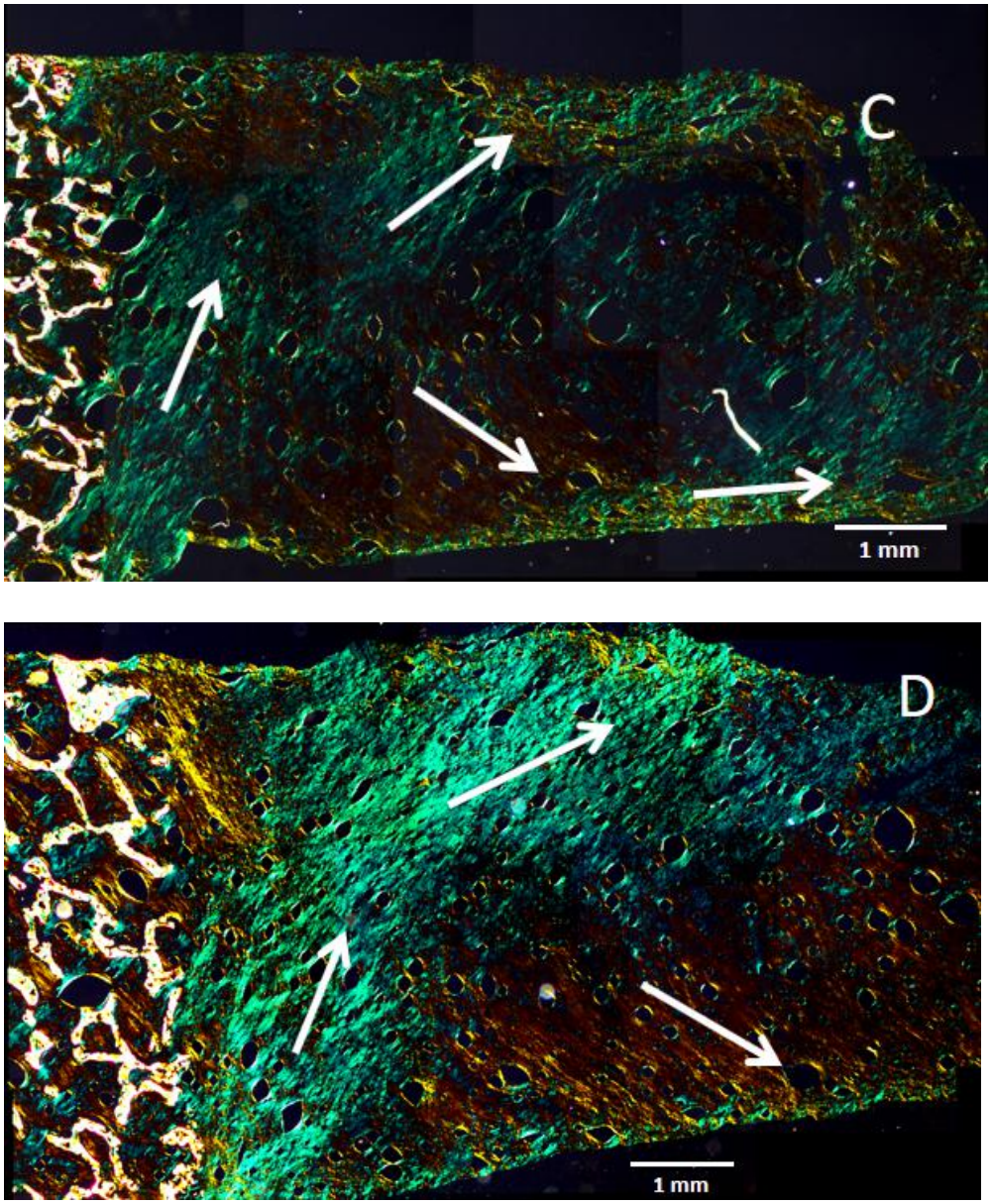

Figure 3.3.2.4. Polarized light images of Picrosirius red staining slides of meniscal enthesis constructs after 4-week culture. A: unstretched construct; B,C,D: stretched constructs. White arrows are used for marking the main orientation of fibers.

Masson's trichrome staining images demonstrate the cell morphology of FCCs in meniscal enthesis constructs. We can find that the cells are elongated along the direction of fiber orientations at interface and collagen region, while they

remain rounded shapes in bone region. Both are found in unstretched constructs and stretched constructs, as cells are elongated mainly along the radial direction at interface region while they turn to longitudinal direction when it comes to the collagen region (Figure 3.3.2.5).

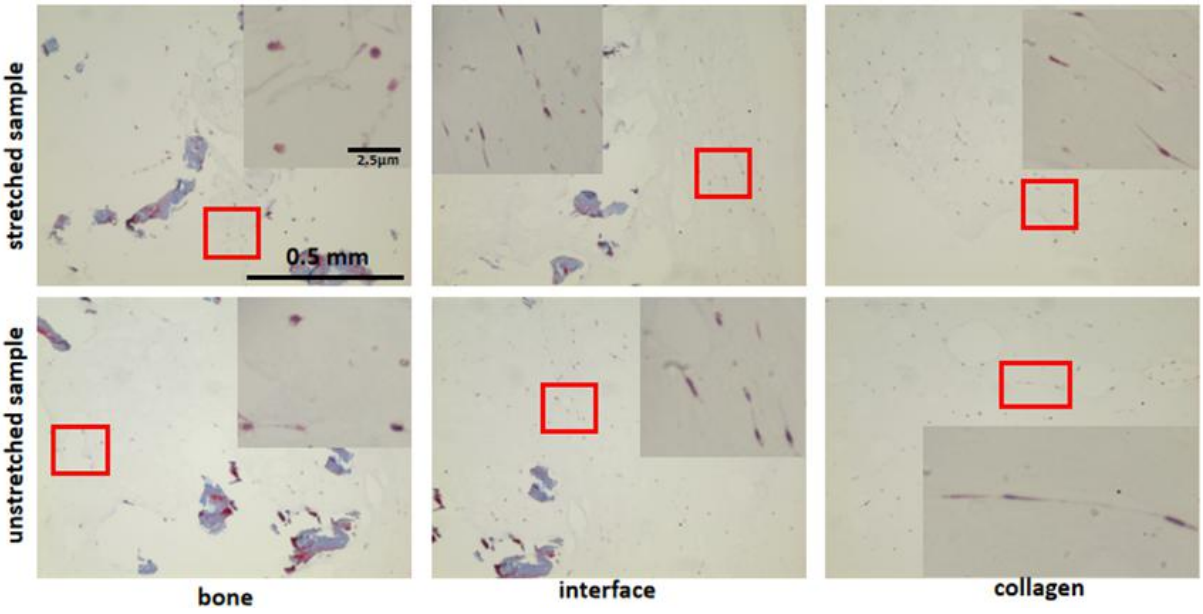

Figure 3.3.2.5. Masson's trichrome staining for cell morphology analysis at bone, interface and collagen regions of unstretched constructs and stretched constructs (cultured for 2 weeks). Red rectangle borders are used to highlight the area of focused cells.

3.3.3 Tensile Testing

Samples from control groups and experimental groups showed different features during stretching to failure process. Still shots of tensile testing process were taken at same time points for comparison between control groups and experimental groups (Figure 3.3.3.1). During necking, it first happened in control

samples (Figure 3.3.3.1 B), then stretching failure started in control samples at interface (Figure 3.3.3.1 C). When control group samples completely failed, necking happened in experimental group samples (Figure 3.3.3.1 D). After that, failure started in experimental group in the middle of collagen (Figure 3.3.3.1 E). This process lasted for long till complete failure in experimental sample in the middle (Figure 3.3.3.1 G).

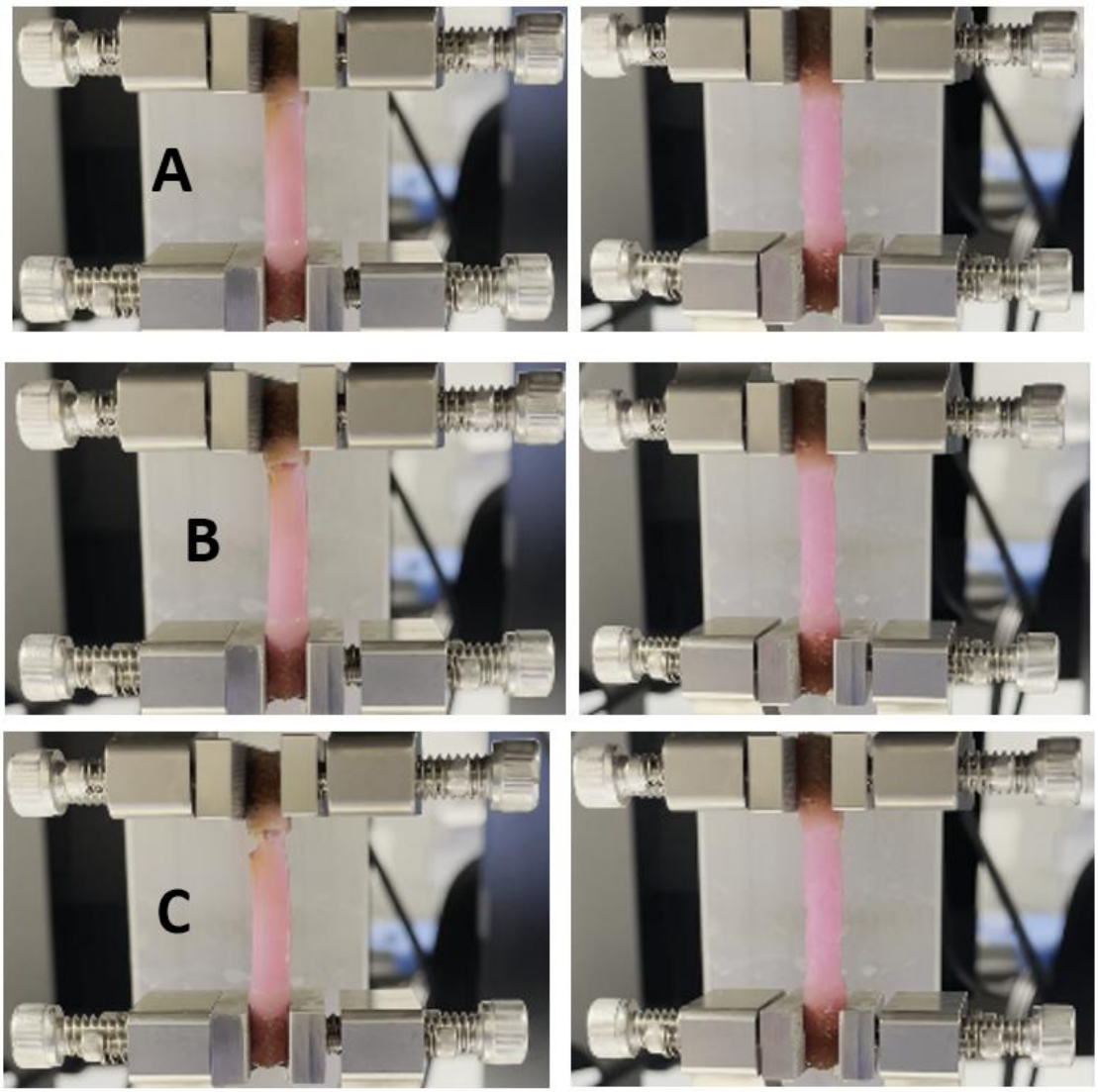

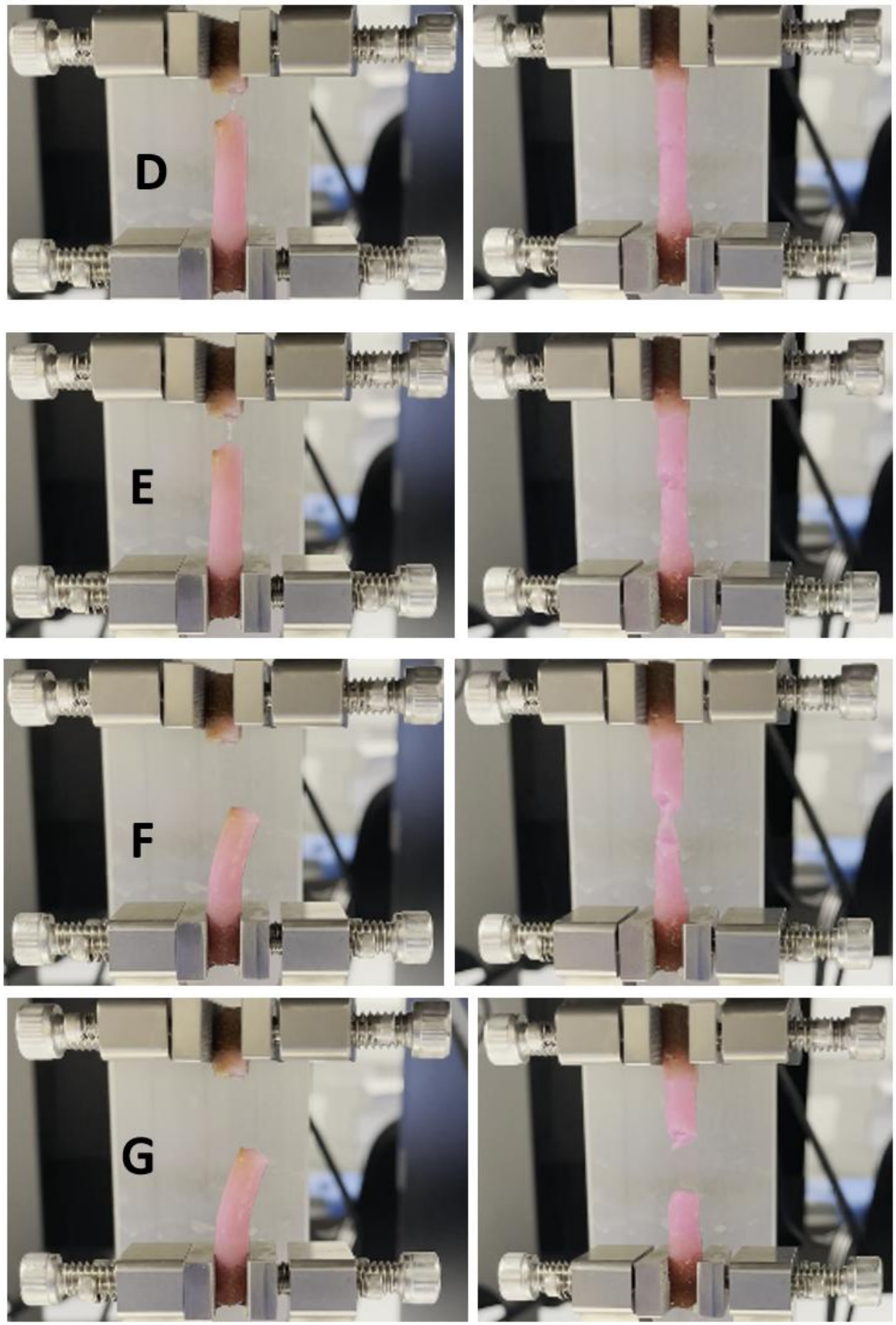

Figure 3.3.3.1. Still shoot images of tensile testing process of unstretched and stretched constructs. Left: unstretched; Right: stretched. A: initial state, initial

length of collagen:~20mm; B: necking in left sample; C: failure started in left sample; D: complete failure in left sample and necking in right sample; E: failure started in right sample; F: failure process of right sample; G: complete failure in right sample.

After collecting and analyzing the tensile testing data, the stress-strain curves of meniscal enthesis constructs from both groups were detained. Obvious differences were observed by comparing curves from control groups and experimental groups. After calculation, the values of different mechanical properties were listed in Table 3.3.3.1. Comparison of UL, UTS, tensile modulus, and strain of failure are compared (Figure 3.3.3.2).

Table 3.3.3.1. Mechanical property data of meniscal enthesis constructs from control groups and experimental groups. * means significant difference ($p<0.05$); + means difference exists ($0.05<p<0.1$).

	* UL (N)	* UTS (N/m^2)	+ Tensile Modulus (Pa)	Toughness (J/m^3)	+ Strain of Failure
Control	0.356±0.19	12986±6218	90528±40262	1272±345	0.266±0.032
Bioreactor	0.203±0.06	8405±2760	56249±22762	1082±598	0.39±0.1

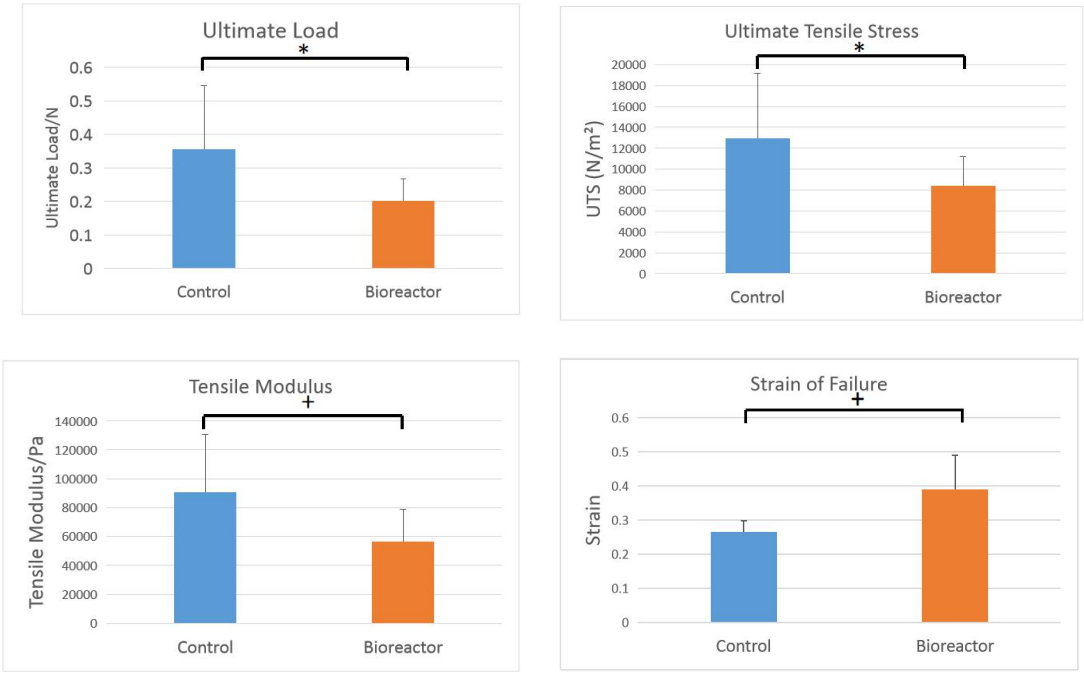

Figure 3.3.3.2. Bar graphs of ultimate load (top left), ultimate tensile stress (top right), tensile modulus (bottom left) and strain of failure (bottom right) between control and bioreactor samples (*significant difference: $p<0.05$; +difference exists: $0.05<p<0.1$).

By comparing the stress-strain curves from control groups and experimental groups, we observed that most of the unstretched constructs showed higher ultimate load (UL), ultimate tensile stress (UTS), and tensile modulus compared to the stretched constructs. However, the stress-strain curves of stretched constructs generally showed the feature of higher strain after the onset of failure during tensile testing compared with control samples (Figure 3.3.3.3).

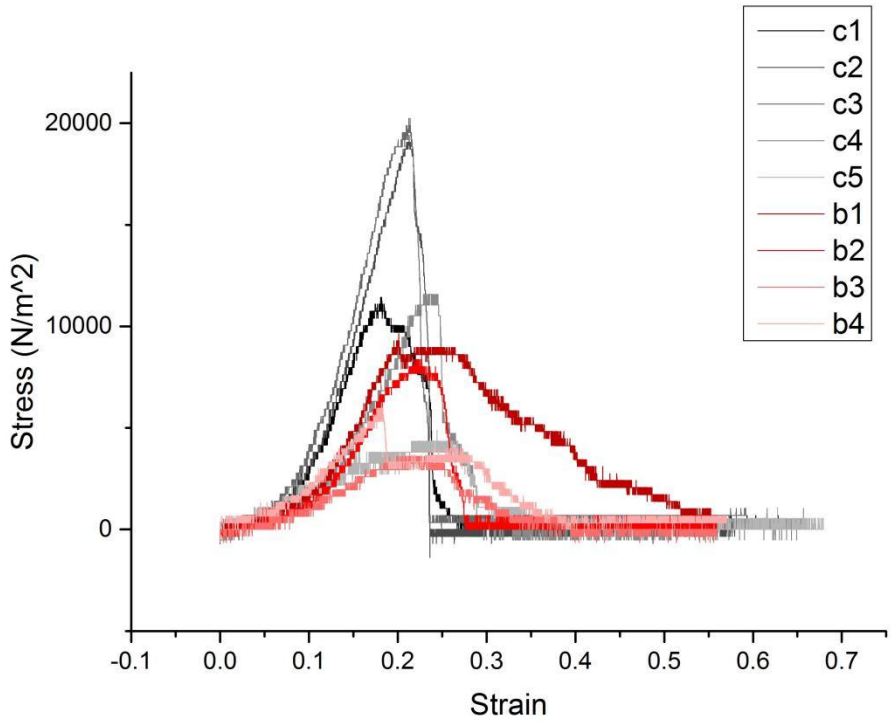

Figure 3.3.3.3. Stress-strain curves of tensile testing data from meniscal enthesis constructs of control and experimental groups. c1-5 are control samples (black series) and b1-4 (red series) are experimental samples.

3.4 Discussion

The aim of this research is to explore the effect of axial stretching stimulation on meniscal enthesis constructs that are clamped and fixed onto bioreactors at both bony ends during culture process. We expected to improve the mechanical properties and fiber organization of meniscal enthesis constructs by stretching stimulation. This provides potential mechanical stimulation and guidance for tissue maturation which can improve the connective integration between bone and soft tissue constructs in tissue engineered meniscus research. In this study, we demonstrated that stretched constructs form more fibers along

longitudinal directions and showed higher strain during tensile testing before complete failure compared with unstretched ones. The stretching effect also resulted in more defects and lower collagen density in meniscal enthesis constructs.

For the realization of stretching function, a 3D printed bioreactor was designed and produced with PLA material. Stretching testing results in the designed bioreactor show that the bioreactor can be manually operated to stretch the sample fixed successfully, and the length of the stretching reached the expected effect of the experiment. At the same time, the normal operation of the culture experiments based on the bioreactor also proves that it has physical and chemical reliability and good biocompatibility, and can be reused. It is worth noting that in the process of designing the bioreactor, we continuously improved the design and introduced different versions of the bioreactor to address the different problems that may occur in the actual experiment, including container sealing, infection, and instrument accuracy. Yet, the process of improvement has not stopped. In fact, even after several versions of the improvements, the current bioreactors still have a lot of room for improvement in terms of material selection and precision. For example, the combination of a TPU series and 3D heat-melt processing is used in 3D printing model to achieve higher resolution-quality[21]. This provides a new idea for improving the precision of bioreactor: the resolution of the stretching bioreactor can be accurate to 0.01 mm or even higher instead of the current 0.1 mm resolution. In this case, slack problem in bioreactors will be better solved and less errors

during stretching process will be caused. Continuous and controllable dynamic stretching function can be achieved in this resolution, which is my further design.

Stretching stimulation on fixed meniscal enthesis constructs along the axial direction successfully guided the formation of collagen fibers along the longitudinal direction, at the same time, decreased the formation of fibers along radial direction. The stretching has provided the enthesis constructs with mechanical signals to cells to guide the formation and remodeling of matrix. As a result, after 4 weeks of culture with stretching, more longitudinal fibers are observed in stretched samples in collagen region, especially at outer edge of collagen zone. Compared to unstretched constructs, the formation of fibers along radial direction obviously decreased. We think that the combination of fibers along radial and longitudinal directions results in higher ultimate load, ultimate tensile stress and tensile modulus in unstretched constructs, as is shown in the tensile testing data. But it is also possible that more defects resulted from stretching stimulation during culture led to the decreased mechanics in experimental group samples, since obviously stretched constructs had more defects than control. More longitudinal fiber formation was associated with larger strain before the stretched constructs' failure. Apart from that, stretched constructs show lower collagen density than the unstretched ones. Signs of partial stretching-induced failure and more local defects can be observed in stretched constructs after 4 weeks of culture. These features, to some extent, have shown us the relationship between structure and function in meniscal enthesis model. In current theories, the movement of

fibers is related to different collagen orientations in the soft tissue region[22]. According to previous research using confocal elastography of the native meniscal enthesis, in the native tissue, away from the interface, collagen fiber bundles move with respect to one another during the initial stages of loading[23]. This is because of the loose combination of fibers with each other. As a result, the fibers will primarily go through rotation and translation along the longitudinal direction instead of being stretched and elongated during the stretching process in culture. The histological images of stretched meniscal enthesis constructs (Figure 3.3.3.1) accorded with this phenomenon: the radial fiber orientations decreased and the longitudinal ones increased compared with unstretched constructs. It was highly possible that the fibers rotated under stretching stimulation from radial to longitudinal direction. The loose combination between fiber bundles also explains for the partial failure or tears phenomenon in collagen part in Figure 3.3.2.2 B and C. Because of the loose combination between fibers, more defects were found in stretched constructs compared with control samples. According to tensile testing data, most stretched constructs with more defects showed lower ultimate load, UTS and tensile modulus compared with control groups. It is highly possible that these defects reduced the organization of fiber bundles in constructs.

Cells were observed to be elongated along the direction of fiber orientation in meniscal enthesis constructs from 2-week cultured samples. This pattern was demonstrated in both the control groups and experimental groups of constructs. At the bone region of constructs, the shape of cells was mainly rounded without

elongation. While at the interface region and collagen region, the cells were a mixture of rounded ones and elongated ones. And the elongated cells are deformed along the main orientation of local fiber bundles: at interface region, cells were mainly elongated along the edge of interface, which is the radial direction. While at collagen region, cells were mainly elongated along longitudinal direction. This finding is consistent with the previous research on clamping effect[24]. As we know, the mechanical stimulation functions as a basic regulator of tissue homeostasis. Tissues will modify their composition and mechanical properties as a response to the mechanical stimulation[25]. For cells, the mechanical signals can influence the cell morphology. Similar phenomenon of cell reorientation after direction stretching stimulation has been found in previous research[26-29]. The elongated cells can also be used an auxiliary tool to help us define the orientation of fiber bundles.

3.5 Conclusions

In this study, the bioreactor I designed and produced with 3D printing using PLA material successfully stretched the meniscal enthesis constructs to expected length without observable necking, which indicates the successful introduction of stretching stimulation. For the effect of axial stretching stimulation, the seeded FCCs were elongated in the direction of fiber orientation. The formation of more fibers along longitudinal direction and less along radial direction in stretched constructs is guided by the axial stretching stimulation compared with unstretched constructs. The stretching stimulation also brings in lower collagen density and more local defects in collagen, which accounts for the lower ultimate load, ultimate

tensile stress and tensile modulus compared to fixed constructs without stretching stimulation. However, the stretching effect results in higher strain before the failure of constructs by 50% compared to constructs without stretching.

3.6 References

1. Messner, K. and Gao, J. The menisci of the knee joint. anatomical and functional characteristics, and a rationale for clinical treatment. *J Anat*, 1998. 193(Pt 2), pp. 161-178.
2. Benjamin, M., Evans, E. J., Rao, R. D., Findlay, J. A. and Pemberton, D. J. Quantitative differences in the histology of the attachment zones of the meniscal horns in the knee joint of man. *Journal of Anatom*y, 1991. 177, pp. 127-134.
3. Makris, E. A., Hadidi, P. and Athanasiou, K. A. The knee meniscus: structure–function, pathophysiology, current repair techniques, and prospects for regeneration. *Biomaterials*, 2011. 32(30), pp. 7411-7431.
4. Setton, L. A. Guilak, F., Hsu, E. W. and Vail, T. P. Biomechanical factors in tissue engineered meniscal repair. *Clin Orthop Relat Res*, 1999. 367(Suppl. l), pp. S254-S272.
5. Villegas, D. F. and Haut Donahue, T. L. Donahue Collagen morphology in human meniscal attachments: a SEM study. *Connect Tissue Res*., 2010. 51(5), pp. 327-336.
6. Villegas, D. F., Hansen, T. A., Liu, D. F., and Haut Donahue, T. L. A quantitative study of the microstructure and biochemistry of the medial meniscal horn attachments. *Ann Biomed Eng*., 2008. 36(1), pp. 123-131.

7. Shaw, H. M. and Benjamin, M. Structure–function relationships of entheses in relation to mechanical load and exercise. *Scand J Med Sci Sports*, 2007. 17(4), pp. 303-315.
8. Donahue, T. L. H., Hull, M. L., Rashid, M. M. and Jacobs, C. R. How the stiffness of meniscal attachments and meniscal material properties affect tibio-femoral contact pressure computed using a validated finite element model of the human knee joint. *Journal of biomechanics*, 2003. 36(1), pp. 19-34.
9. Jones, A. O., Houang, M. T. W., Low, R. S. and Wood, D. G. Medial meniscus posterior root attachment injury and degeneration: MRI findings. *Australasian radiology*, 2006. 50(4), pp. 306-313.
10. Abraham, A. C., Pauly, H. M. and Donahue, T. L. H. Deleterious effects of osteoarthritis on the structure and function of the meniscal enthesis. *Osteoarthritis and Cartilage*, 2014. 22(2), pp. 275-283.
11. Kester, C. R., Iii, P. E. C. and Pearson, S. E. Lateral meniscal allograft transplant: Dovetail bone bridge preparation. *Arthroscopy Techniques*, 2021. 10(4), pp. e969-e973.
12. Khetia, E. A. and McKeon, B. P. Meniscal allografts: biomechanics and techniques. *Sports Med. Arthrosc*. 2007. 15, pp. 114–120.
13. Boys, A., Bonassar, L. and Estroff, L. Next generation tissue engineering of orthopedic soft tissue-to-bone interfaces. MRS Commun., 2017. 7(3), pp. 289-308.

14. Villegas, D. F., Hansen, T. A., Liu, D. F. and Haut Donahue, T. L. A quantitative study of the microstructure and biochemistry of the medial meniscal horn attachments. *Ann. Biomed. Eng.* 2008. 36, pp. 123-131.
15. Villegas, D. F. and Haut Donahue, T. L. Collagen morphology in human meniscal attachments: a SEM study. Connect. *Tissue Res*. 2010. 51, pp. 327-336.
16. Villegas, D. F., Maes, J. A., Magee, S. D. and Haut Donahue, T. L. Failure properties and strain distribution analysis of meniscal attachments. *J. Biomech*. 2007. 40, pp. 2655–2662.
17. Hu, Y., Birman, V., Demyier-Black, A., Schwartz, A. G., Thomopoulos, S. and Genin, G. M. Stochastic interdigitation as a toughening mechanism at the interface between tendon and bone. *Biophys. J.*, 2015. 108, pp. 431-437.
18. Abraham, A. C. and Haut Donahue, T. L. From meniscus to bone: a quantitative evaluation of structure and function of the human meniscal attachments. *Acta Biomater.* 2013. 9, pp. 6322-6329.
19. Moffat, K. L., Sun, W-H. S., Pena, P. E., Chahine, N. O., Doty, S. B., Ateshian, G. A., Hung, C. T. and Lu, H. H. Characterization of the structure-function relationship at the ligament-to-bone interface. *Proc. Natl. Acad. Sci. U.S.A*. 2008. 105, pp. 7947-7952.
20. Puetzer, J. L. and Bonassar, L. J. Physiologically distributed loading patterns drive the formation of zonally organized collagen structures in tissue engineered meniscus. *Tissue Eng*. 2016. A 22, pp. 907-916.

21. McCorry, M., Mansfield, M. and Bonassar, L. A model system for developing a tissue engineered meniscal enthesis. Acta Biomater, 2017. 56, pp. 110-117.

22. Kang, K. S., Jee, C., Bae, J. H., Jung, H. J., & Huh, P. H. (2019). Heat capacity variables of thermoplastic polyurethane for high-quality 3D printing resolution and their characteristics. Materials Letters, 257, 126698.

23. J.J. Ballyns, J.P. Gleghorn, V. Niebrzydowski, J.J. Rawlinson, H.G. Potter, S.A.Maher, T.M. Wright, L.J. Bonassar, Image-guided tissue engineering of anatomically shaped implants via MRI and micro-CT using injection molding, Tissue Eng. Part A 14 (2008) 1195 – 1202.

24. Genin, G. M. and Thomopoulos, S. The Tendon-to-Bone Attachment: Unification through Disarray. *Nat. Mater.*, 2017. 16, pp. 607-608.

25. Boys, A. J., Kunitake, J. A. M. R., Henak, C. R., Cohen, I., Estroff, L. A. and Bonassar, L. J. Understanding the stiff-to-compliant transition of the meniscal attachments by spatial correlation of composition, structure, and mechanics. *ACS Applied Materials and Interfaces*, 2019. 11(30), pp. 26559-26570.

26. McCorry, M. C., Mansfield, M. M., Sha, X., Coppola, D. J., Lee, J. W., & Bonassar, L. J. (2017). A model system for developing a tissue engineered meniscal enthesis. Acta Biomaterialia, 56, 110 – 117.

27. Zhang, L., Kahn, C. J. F., Chen, H. Q., Tran, N., & Wang, X. (2008). Effect of uniaxial stretching on rat bone mesenchymal stem cell: Orientation and expressions of collagen types I and III and tenascin-C. Cell Biology International, 32(3), 344 – 352.

28. M. Chiba, H. Mitani Cytoskeletal changes and the system of regulation of alkaline phosphatase activity in human periodontal ligament cells induced by mechanical stress Cell Biochem Funct, 22 (2004), pp. 249-256.
29. R. Chiquet-Ehrismann, R.P. Tucker Connective tissues: signalling by tenascins Int J Biochem Cell Biol, 36 (2004), pp. 1085-1089.
30. S.G. Kim, T. Akaike, T. Sasagaw, Y. Atomi, H. Kurosawa Gene expression of type I and type III collagen by mechanical stretch in anterior cruciate ligament cells Cell Struct Funct, 27 (2002), pp. 139-144.
31. R.M. McAdams, S.B. Mustafa, J.S. Shenberger, P.S. Dixon, B.M. Henson, R.J. DiGeronimo Cyclic stretch attenuates effects of hyperoxia on cell proliferation and viability in human alveolar epithelial cells Am J Physiol Lung Cell Mol Physiol, 291 (2006), pp. L166-L174.

CHAPTER 4. LIMITATIONS AND FUTURE WORK

There are still some limitations in the research process that need to be addressed in subsequent studies. We have already known that mechanical stimuli are crucial for the normal structures and functions of tissues[1], especially in tissue engineering research. The appropriate rate of mechanical stimulation is a critical factor involved. Several studies have already demonstrated that the use of dynamic culture devices providing adequate mechanical stimuli with suitable stimulating rate will bring in significant improvements in structural and functional tissue maturation[2,3,4]. However, due to the experimental cycle and technical limitations, the exploration of the stretching rate in this study is still in its infancy, and the change of stretching rate from 45° rotation every 3 to 6 days still leads to partial failure in collagen of meniscal enthesis constructs. A more gradual and appropriate stretching method is in need to be explored as one of the future directions.

Culture time before the applying of stretching to constructs is another potential influence factor to the connective integration at interface, besides the mechanical stimulation rate. Related research has been applied on mesenchymal stem cells(MSCs). Azim et al. demonstrated that culture time is an important factor for tissue mechanical properties and cells' gene expression[5]. In this study, a two-way interaction effect has been found between culture time and substrate topography after 14 days' culture on tissue. And a huge decrease in Young's modulus of tissue on day 7 is also observed compared to day 1[6]. In summary, the time span during which the cells are seeded and cultured is seen as a critical factor

for altering mechanical properties. This conclusion can also serve as a future direction for our study. The 5-day culture time before stretching can be adjusted for future exploration in order to provide more mature collagen formation. It can hopefully decrease the local defects and partial failure phenomenon during stretching process.

Apart from axial stretching stimulation, more complex mechanical loading which is more similar to the native loading environment in human knee joint is expected to be applied onto meniscal enthesis constructs. As has been introduced, the native meniscal enthesis is subjected to a very complex loading environment during our daily exercise and movement, and the axial tensile fore is only part of the loading stimulation. For the future research, anatomically accurate tissue engineered menisci[7,8] or curved meniscal enthesis construct models can be used as the experimental and testing model to better mimic the native meniscus geometry. Not only axial direction stretching, but more mechanical stimulation in different directions can be applied to the model in an attempt to research the culture results after culture.

In addition, the currently used 3D printing still has room on manufacturing accuracy for improvement. A variety of high resolution additive manufacturing methods, for example, stereolithography (SLA)[9-11], in bioreactor design process can be considered and tried out in future in order to improve the surface precision of printing devices. In this case we can decrease the errors raised from slack or slippery in mechanically connected devices. Another limitation is on the manual

operation on stretching bioreactors. The manual operation of the stretching process is not as accurate and controllable as expected, which will also bring in higher risk of infection into sterile conditions. We are trying to design and apply remote control system into the bioreactor design (e.g., motor step driving). In this case, a more consistent, accurate stretching method will be introduced, and the problem of manual stretching induced possibility of infection will be decrease. This also opens up the possibility of exploring more moderate stretching rates.

References

1. Putame, G., Gabetti, S., Carbonaro, D., Meglio, F. Di, Romano, V., Sacco, A. M., Belviso, I., Serino, G., Bignardi, C., Morbiducci, U., Castaldo, C and Massai, D. Compact and tunable stretch bioreactor advancing tissue engineering implementation. Application to engineered cardiac constructs. *Medical Engineering and Physics*, 2010. 84, pp. 1-9.
2. Powell, C. A., Smiley, B. L., Mills, J. and Vandenburgh, H. H. Mechanical stimulation improves tissue-engineered human skeletal muscle. *Am J Physiol Physiol*, 2002. 283, pp. C1557-C1565.
3. Moon, D. G., Christ, G., Stitzel, J. D., Atala, A. and Yoo, J. J. Cyclic mechanical preconditioning improves engineered muscle contraction. Tissue Engineering Part A, 2008. 14(4), pp. 473-482.
4. Somers, S. M., Spector, A. A., DiGirolamo, D. J. and Grayson, W. L. Biophysical stimulation for engineering functional skeletal muscle. *Tissue Engineering Part B: Reviews*, 2017. 23(4), pp. 362-372.
5. Parandakh, A., Anbarlou, A., & Tafazzoli-shadpour, M. (2019). Colloids and Surfaces B : Biointerfaces Substrate topography interacts with substrate sti ff ness and culture time to regulate mechanical properties and smooth muscle di ff erentiation of mesenchymal stem cells. Colloids and Surfaces B: Biointerfaces, 173(September 2018), 194 – 201.
6. E.M. Darling, P.E. Pritchett, B.A. Evans, R. Superfine, S. Zauscher, F. Guilak Mechanical properties and gene expression of chondrocytes on micropatterned

substrates following dedifferentiation in monolayer Cell. Mol. Bioeng., 2 (2009), pp. 395-404.

7. J.J. Ballyns, J.P. Gleghorn, V. Niebrzydowski, J.J. Rawlinson, H.G. Potter, S.A. Maher, T.M. Wright, L.J. Bonassar, Image-guided tissue engineering of anatomically shaped implants via MRI and micro-CT using injection molding, Tissue Eng. Part A 14 (2008) 1195 – 1202.
8. J.L. Puetzer, E. Koo, L.J. Bonassar, Induction of fiber alignment and mechanical anisotropy in tissue engineered menisci with mechanical anchoring, J. Biomech. 48 (2015) 1436 – 1443.
9. Arslan, A., Steiger, W., Roose, P., Van den Bergen, H., Gruber, P., Zerobin, E., Gantner, F., Guillaume, O., Ovsianikov, A., Van Vlierberghe, S. and Dubruel, P. Polymer architecture as key to unprecedented high-resolution 3D-printing performance: The case of biodegradable hexa-functional telechelic urethane-based poly-ε-caprolactone. *Materials Today*, 2021. 44(April), pp. 25-39.
10. Fullerton, J. N., Frodsham, G. C. and Day, R. M. 3D printing for the many, not the few. *Nat. Biotech.*, 2014. 32(11), pp. 1086-1087.
11. Sotov, A., Kantyukov, A., Popovich, A. and Sufiiarov, V. LCD-SLA 3D printing of BaTiO 3 piezoelectric ceramics. 2021 July.

APPENDIX 1: SUPPLEMENTAL FIGURES

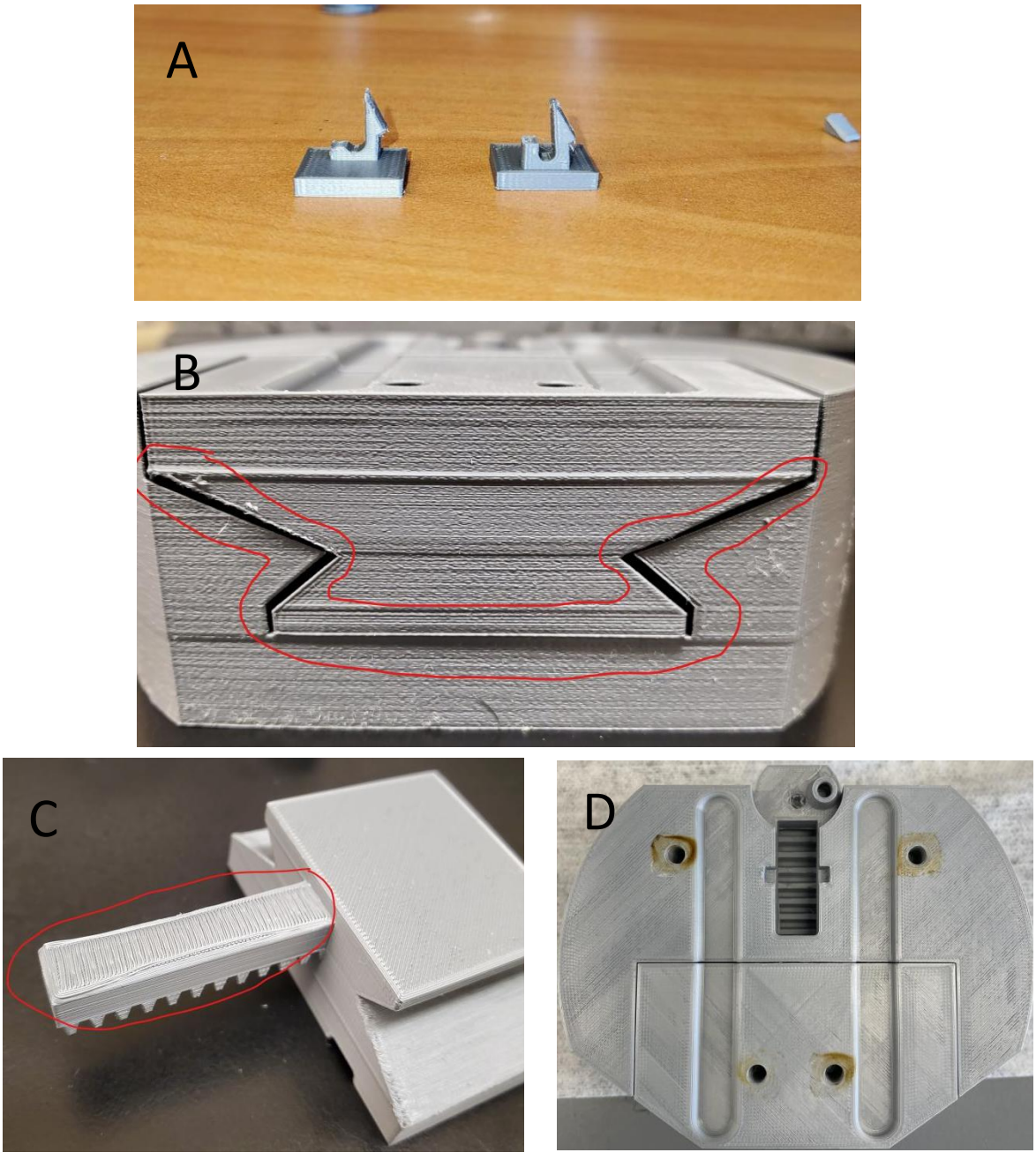

Figure S1. Failed printing and structure during bioreactor design and testing. A: broken snap-lock structure; B: rough surface of 3D printing bioreactor; C: curved rack structure; D: broken screw connection structure.

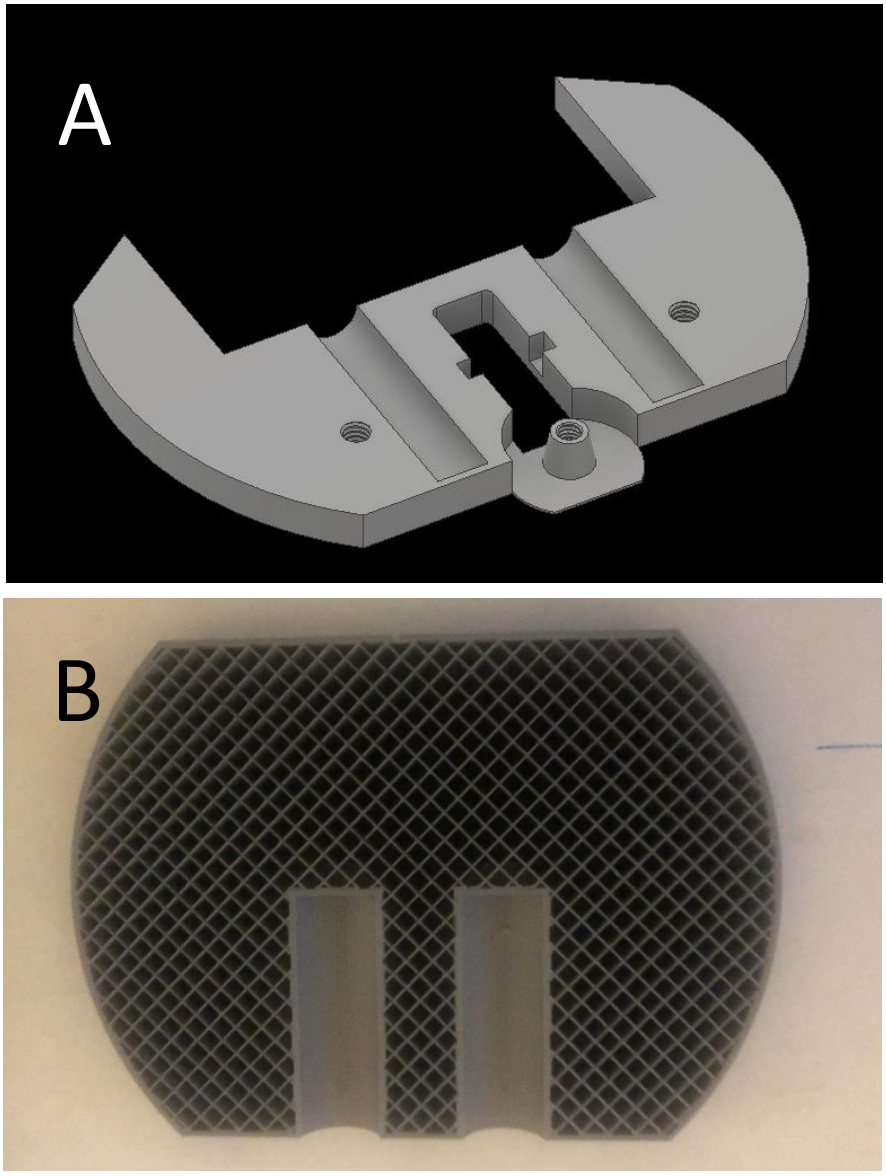

Figure S2. Images of components of 3D printed bioreactor. A: cylindrical chamber and reinforced screw connection structure in version5 bioreactor; B: inner cross-grid network structure of 3D printed bioreactor

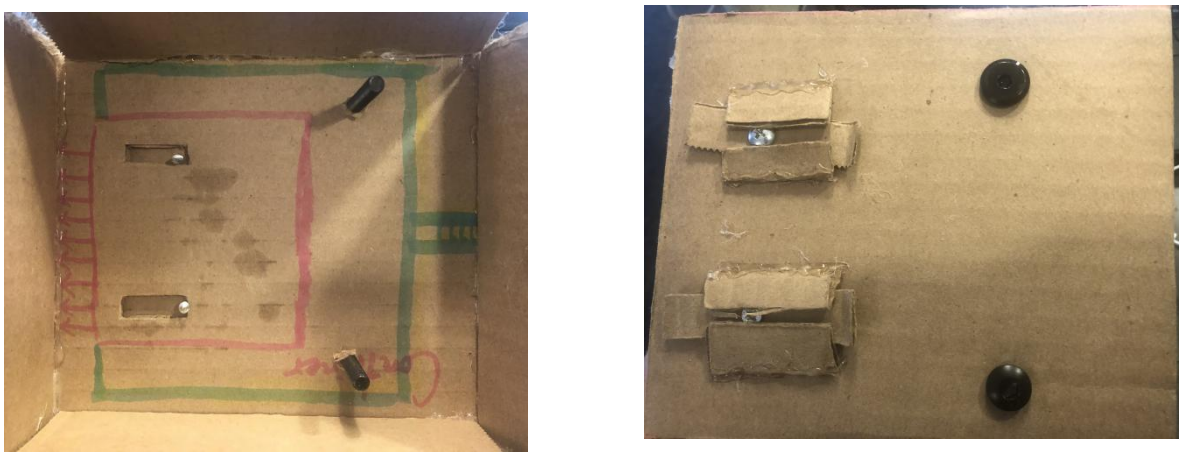

Figure S3. Images of cardboard model for micrometer head-driven bioreactor design. Left: top view; Right: upward view.

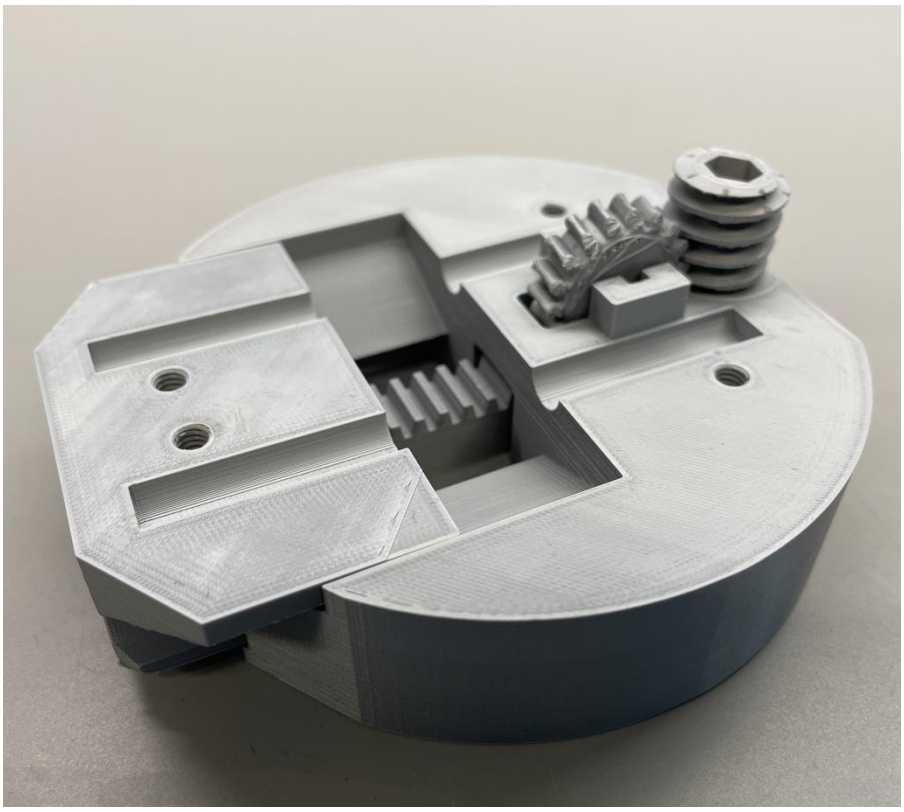

Figure S4. Image of currently used bioreactor for culture with stretching.

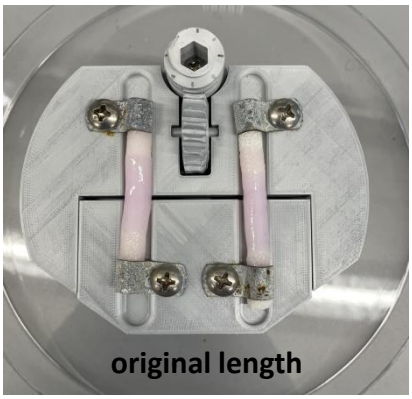
original length

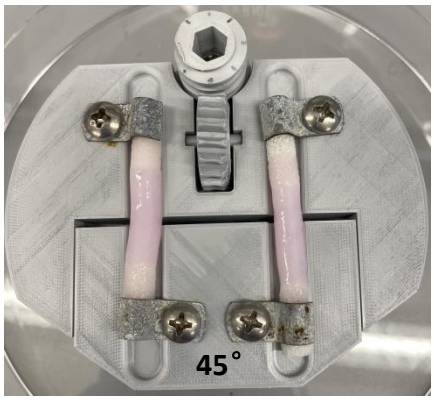
45°

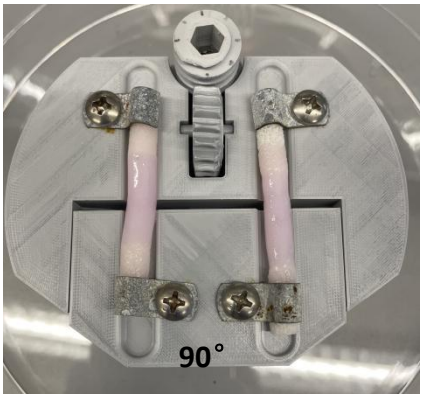
90°

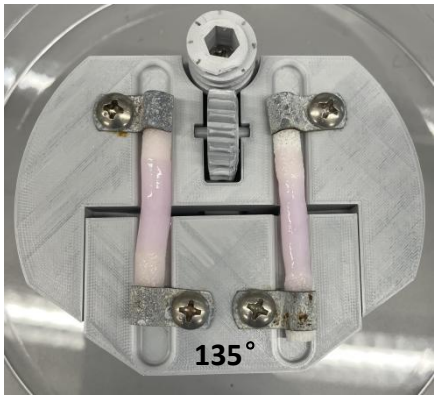
135°


180°

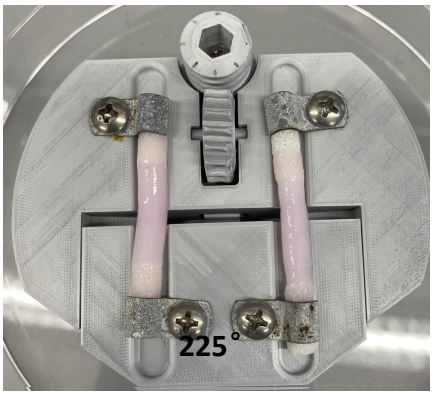
225°


270°


315°

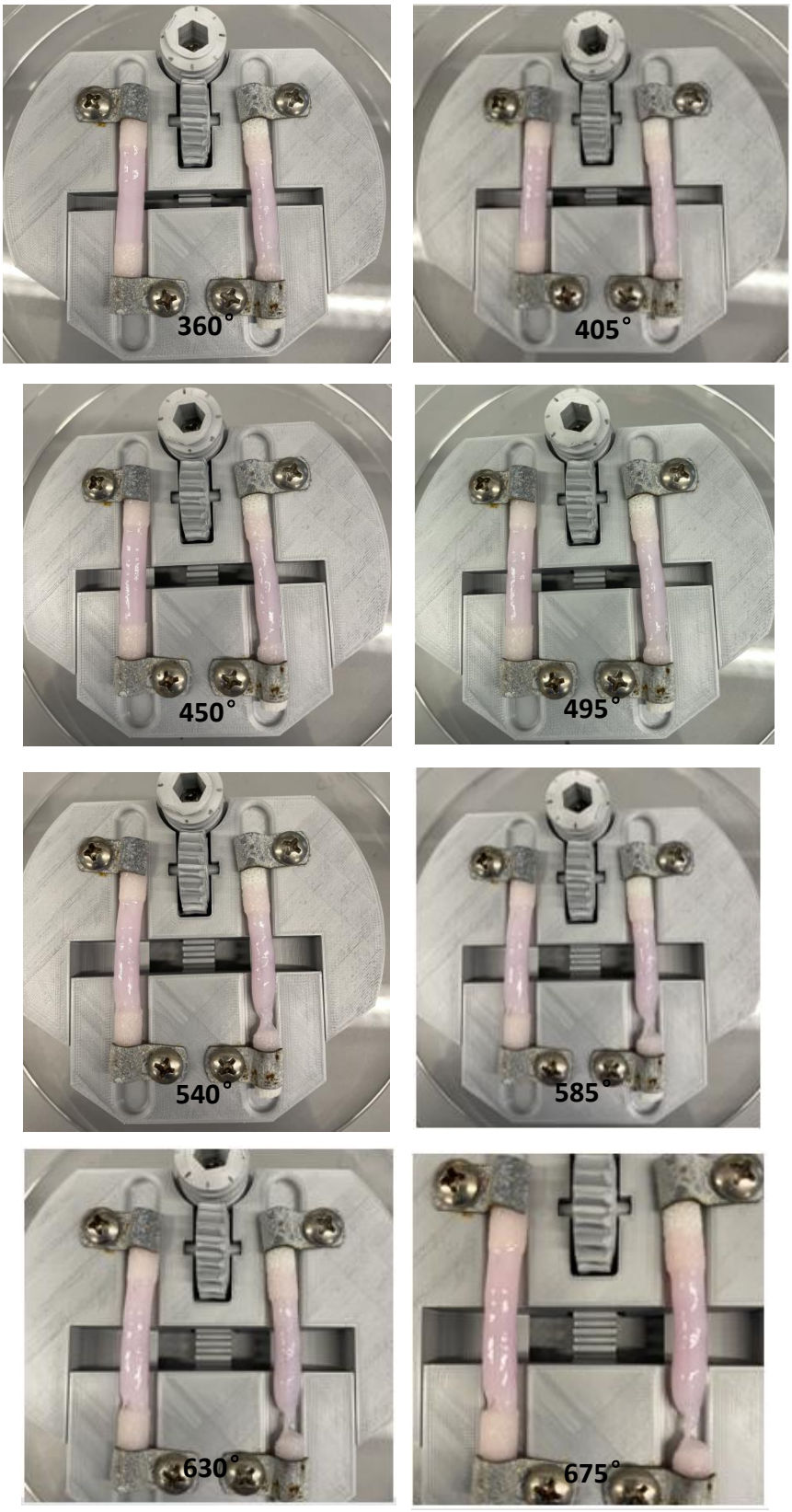

Figure S5. Images of meniscal enthesis constructs on stretching bioreactors during stretching-to-failure testing for bioreactors

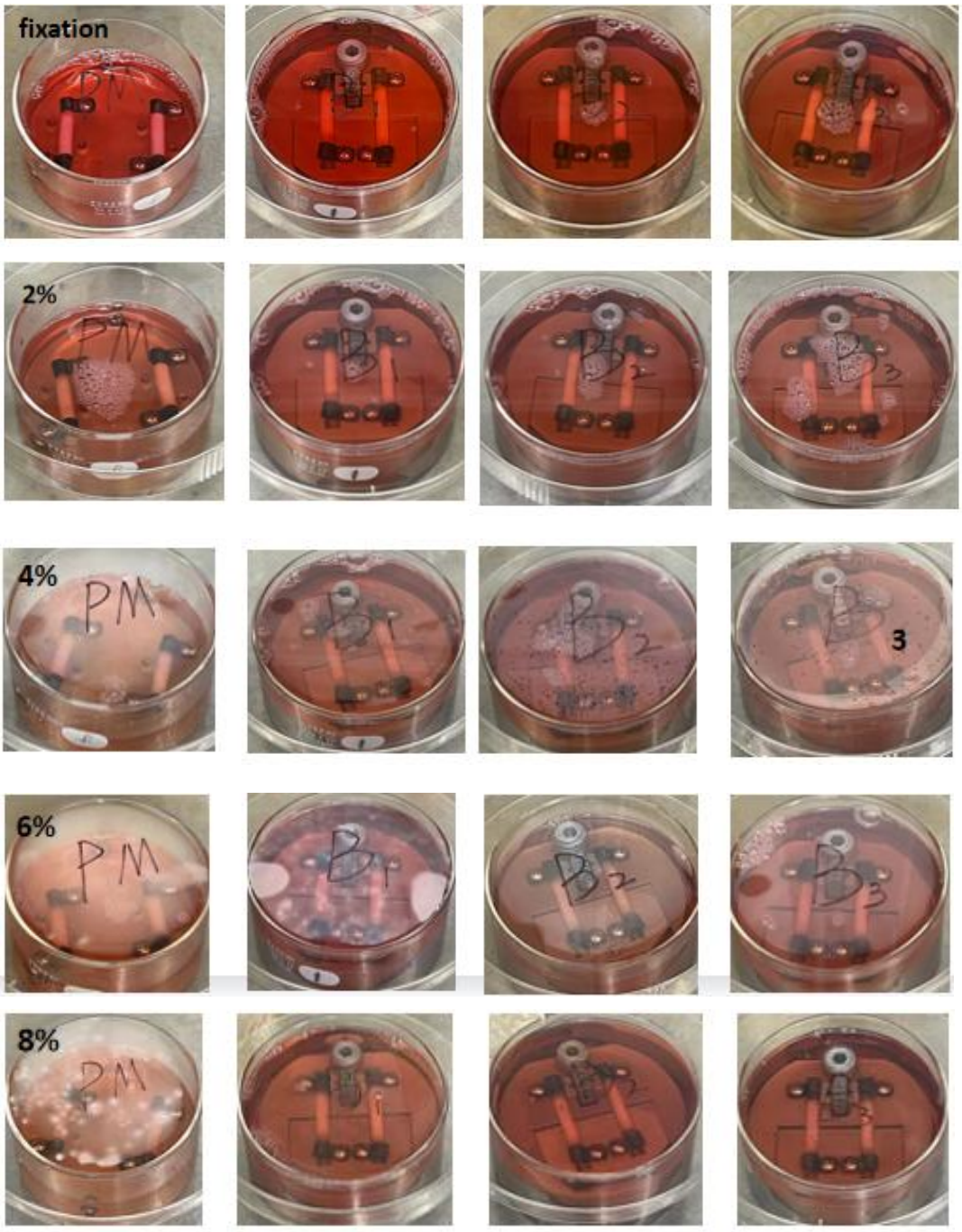

Figure S6. Images of meniscal enthesis constructs during 4-week culture. From top line to bottom: constructs fixation, 2%, 4%, 6%, 8% stretching; From left column to right: control, bioreactor1, bioreactor2, bioreactor3.

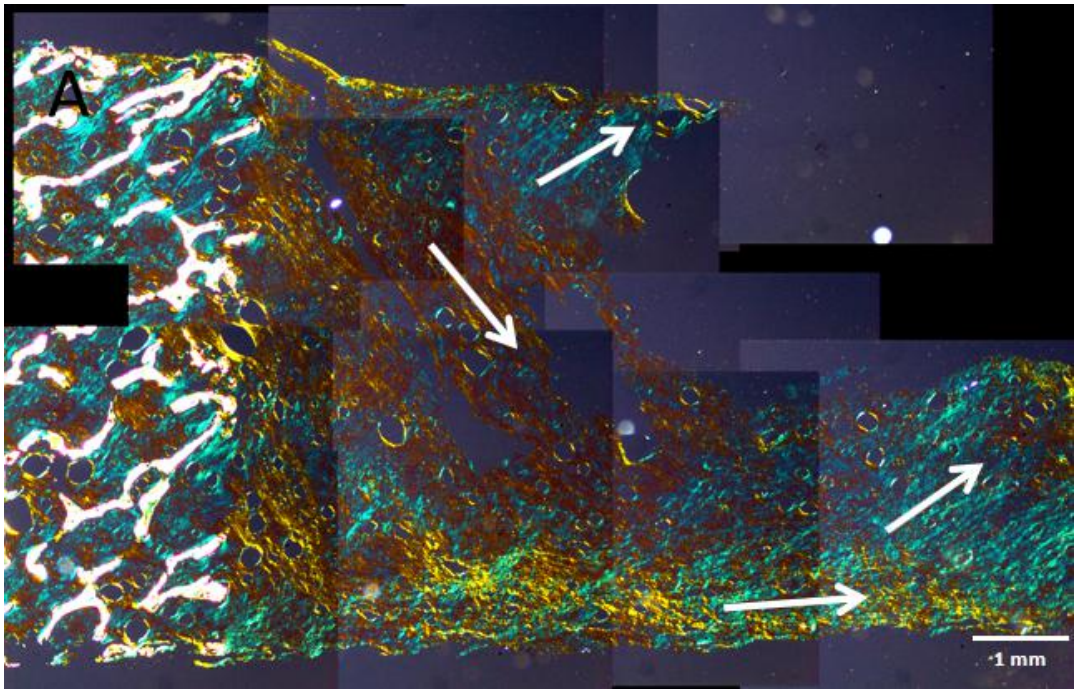
A
1 mm

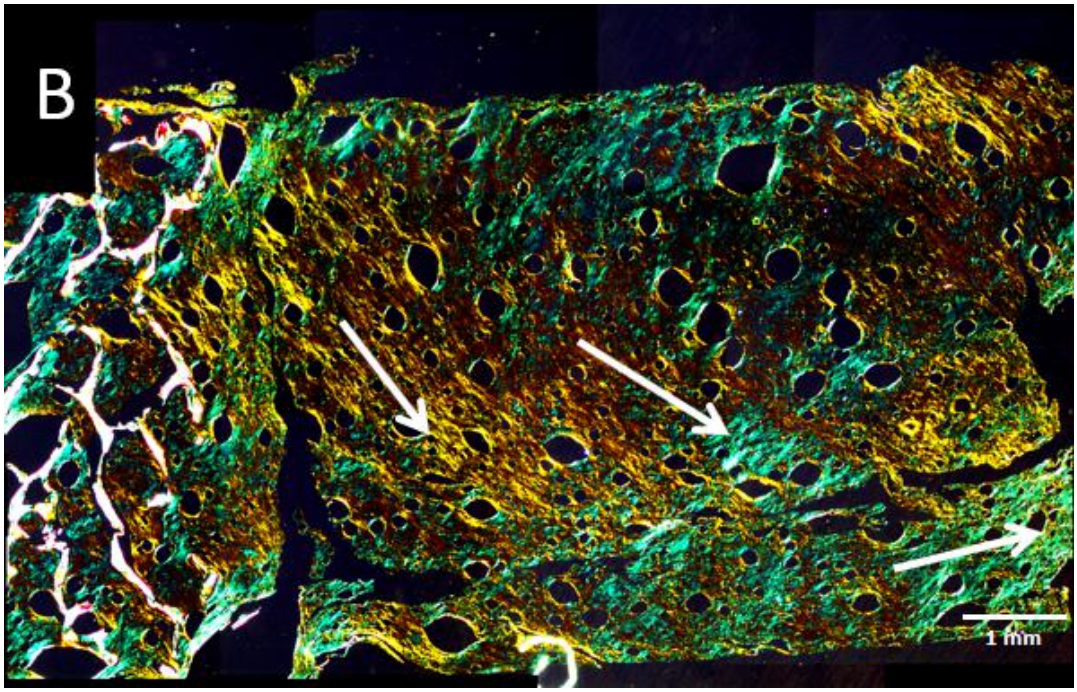
B
1 mm

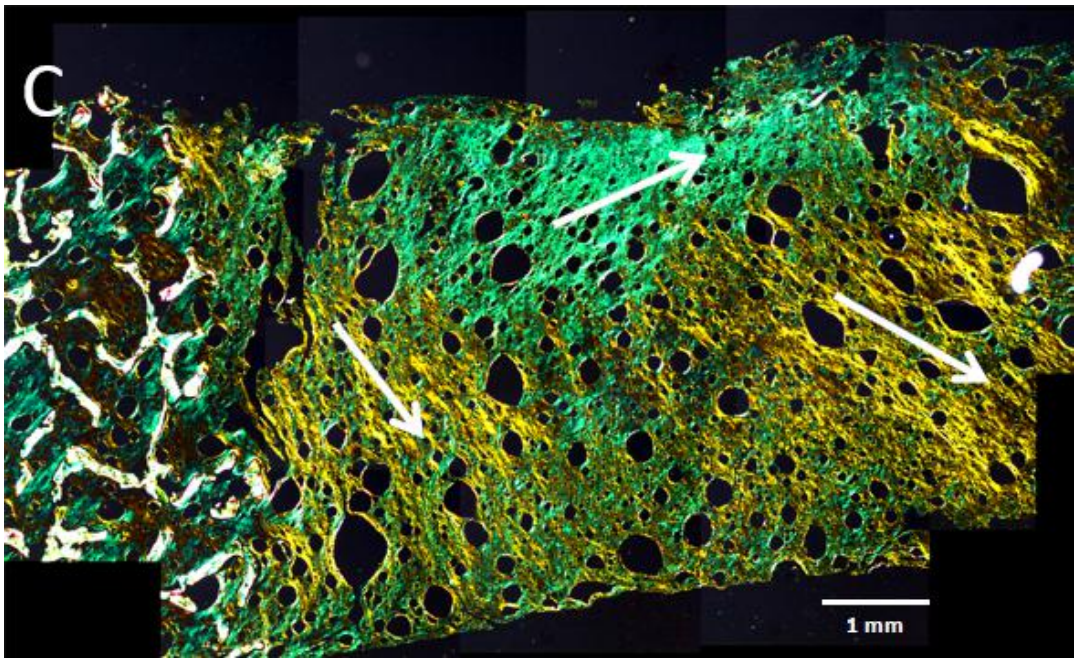

Figure S7. Polarized light images of 4-week stretched meniscal enthesis constructs. A: sample bioreactor2; B,C: samples from bioreactor3. The white arrows show the main direction of the fiber bundles.

APPENDIX 2: SUPPENTAL TABLES

degree	distance(mm)			
0	1.25	1.59	0.99	1.4
45°	1.71	1.96	1.5	1.82
90°	2.26	2.53	1.94	2.28
135°	2.58	2.83	2.36	2.71
180°	3.06	3.27	2.78	3.1
225°	3.44	3.79	3.11	3.58
270°	3.95	4.31	3.57	4.05
315°	4.2	4.57	4.13	4.23
360°	4.48	4.96	4.43	4.78
total distance	**3.23**	**3.37**	**3.44**	**3.38**

degree	distance(mm)			
0	1.17	0.96	1.17	1.36
45°	1.67	1.39	1.71	1.69
90°	1.99	1.9	2.1	2.22
135°	2.48	2.55	2.51	2.57
180°	2.82	2.86	2.85	2.89
225°	3.25	3.27	3.29	3.25
270°	3.56	3.58	3.56	3.81
315°	4.13	4.11	4.19	4.16
360°	4.5	4.45	4.53	4.84
total distance	**3.33**	**3.49**	**3.36**	**3.48**

Supplement Table S1. Stretched distance testing data from bioreactor. The stretch-out distances were measured and recorded for every 45° of rotation for stretching testing.The bioreactor was rotated for 360° in total.